S- and *P*-wave fully strange tetraquark states from QCD sum rules

Niu Su and Hua-Xing Chen*

School of Physics, Southeast University, Nanjing 210094, China

(Received 6 May 2022; accepted 12 July 2022; published 26 July 2022)

We apply the QCD sum rule method to systematically study the *S*- and *P*-wave fully strange tetraquark states within the diquark-antidiquark picture. We systematically construct their interpolating currents by explicitly adding the covariant derivative operator. Our results suggest that the $f_0(2100)$, $X(2063)$, and $f_2(2010)$ may be explained as the *S*-wave $ss\bar{s}\bar{s}$ tetraquark states with the quantum numbers $J^{PC}=0^{++}$, 1^{+-}, and 2^{++}, respectively. Our results also suggest that both the $X(2370)$ and $X(2500)$ may be explained as the *P*-wave $ss\bar{s}\bar{s}$ tetraquark states of $J^{PC}=0^{-+}$, and both the $\phi(2170)$ and $X(2400)$ may be explained as the *P*-wave $ss\bar{s}\bar{s}$ tetraquark states of $J^{PC}=1^{--}$. The masses of the $ss\bar{s}\bar{s}$ tetraquark states with the exotic quantum number $J^{PC}=1^{-+}$ are extracted from two noncorrelated currents to be $2.45^{+0.20}_{-0.25}$ GeV and $2.49^{+0.21}_{-0.25}$ GeV.

DOI: 10.1103/PhysRevD.106.014023

I. INTRODUCTION

In the past 20 years many exotic hadrons were observed in experiments [1], which bring us the renaissance of the hadron spectroscopy [2–22]. Some of them are good candidates for the fully strange tetraquark states, which contain many strangeness components. Experimentally, their widths are possibly not too broad, so they are capable of being observed. Theoretically, their internal structures are simpler than other multiquark states due to the Pauli principle restricting identical strangeness quarks/antiquarks. This limits their potential number and makes them easier to be observed.

There have been some rich-strangeness signals observed at around 2.0 GeV, for example,

(i) In 2006 the *BABAR* Collaboration observed the $\phi(2170)/Y(2175)$ in the $e^+e^-\to\phi f_0(980)$ process [23].

(ii) In 2010 the BESIII Collaboration observed the $X(2120)$ and $X(2370)$ in the $\pi\pi\eta'$ invariant mass spectrum of the $J/\psi\to\gamma\pi\pi\eta'$ decay [24]. Later in 2019 they confirmed the $X(2370)$ in the $K\bar{K}\eta'$ invariant mass spectrum of the $J/\psi\to\gamma K\bar{K}\eta'$ decay, but they did not observe the $X(2120)$ in this process [25]. This suggests that the $X(2370)$ contains more strangeness components.

(iii) In 2016 the BESIII Collaboration performed a partial wave analysis of the $J/\psi\to\gamma\phi\phi$ decay [26], where they observed one scalar resonance $f_0(2100)$, one pseudoscalar resonance $X(2500)$, as well as three tensor resonances $f_2(2010)$, $f_2(2300)$, and $f_2(2340)$ in the $\phi\phi$ invariant mass spectrum.

(iv) In 2018 the BESIII Collaboration observed the $X(2063)$ in the $\phi\eta'$ invariant mass spectrum of the $J/\psi\to\phi\eta\eta'$ decay [27].

With a large amount of the J/ψ sample, the BESIII Collaboration is still carefully examining the physics happening at around 2.0 GeV, and more rich-strangeness signals are expected in the coming future. Such experiments can also be performed by the Belle-II, COMPASS, and GlueX Collaborations, etc.

In the past years we have applied the QCD sum rule method to study the $ss\bar{s}\bar{s}$ tetraquark states, separately for the states with the quantum numbers $J^{PC}=0^{-+}/1^{+-}/1^{--}/4^{+-}$ [28–32]. Relevant QCD sum rule studies and quark model calculations can be found in Refs. [33–42]. Especially, a thorough quark model calculation was performed in Ref. [38] to systematically study the $1S$-, $1P$-, and $2S$-wave $ss\bar{s}\bar{s}$ tetraquark states. We find it useful to perform a similar QCD sum rule study, so in this paper we shall systematically study the $1S$- and $1P$-wave $ss\bar{s}\bar{s}$ tetraquark states using the QCD sum rule method. For simplicity, we denote them as the *S*- and *P*-wave states.

In this paper we shall work within the diquark-antidiquark picture, where the orbital angular momentum can be between the diquark and antidiquark, or it can also be inside the diquark/antidiquark, as depicted in Fig. 1. We call the former λ-mode excitation and the latter ρ-mode excitation. As already classified in Ref. [38], there are altogether four *S*-wave $ss\bar{s}\bar{s}$ states, eight *P*-wave states of

*hxchen@seu.edu.cn

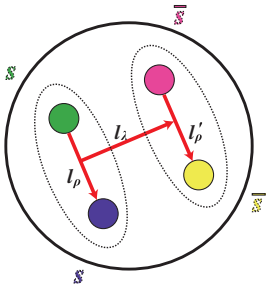

FIG. 1. Relative coordinates $\vec{\lambda}$ and $\vec{\rho}/\vec{\rho}'$ for the diquark-antidiquark system. We use l_λ to denote the orbital angular momentum between the diquark and antidiquark, and l_ρ/l'_ρ to denote the orbital angular momentum inside the diquark/antidiquark.

the λ-mode, and $12P$-wave states of the ρ-mode. We shall systematically construct their interpolating currents by explicitly adding the covariant derivative operator, based on which we shall perform a systematical QCD sum rule study. Note that the tetraquark currents without derivatives were used in our previous QCD sum rule studies [28–31].

Before doing this, we note that the $ss\bar{s}\bar{s}$ tetraquark states are just possible explanations for the rich-strangeness signals observed at around 2.0 GeV, and there exist many other possibilities, for example,

(i) The $\phi(2170)/Y(2175)$ was explained in Refs. [43–48] as a dynamically generated state in the $\phi K\bar{K}/\phi\pi\pi$ systems. Besides, it can also be explained as the 2^3D_1 $s\bar{s}$ meson [49–52], the hidden-strange baryonium state [53–55], and the strangeonium hybrid state [56], etc.

(ii) The $X(2370)$ can be explained as the fourth radial excitation of $\eta(548)/\eta'(958)$ [57], the pseudoscalar glueball [58,59], and their mixing [60]. It can also be explained as the compact hexaquark state of $I^GJ^{PC} = 0^+0^{-+}$ [61] and the hidden-strange baryonium state [62], etc.

(iii) The $X(2500)$ was explained in Refs. [63–67] as the 4^1S_0 or 5^1S_0 $s\bar{s}$ state.

(iv) The $X(2063)$ was explained in Ref. [68] as the second radial excitation of $h_1(1380)$ with $I(J^P) = 0(1^+)$.

We refer to Refs. [69–75] for more lattice QCD studies and Refs. [76–83] for some dynamical analyses.

Another relevant exotic state is the $\eta_1(1855)$ recently observed by BESIII in the $\eta\eta'$ invariant mass spectrum of the $J/\psi \to \gamma\eta\eta'$ decay [84,85]. This resonance has the exotic quantum number $I^GJ^{PC} = 0^+1^{-+}$, which can not be accessed by conventional $\bar{q}q$ mesons. It may be explained as the hybrid meson [86–90] and the $K\bar{K}_1(1400)$ hadronic molecule [91–94], etc. Besides, the $\eta_1(1855)$ may also be explained as the $qs\bar{q}\bar{s}$ $(q = u/d)$ tetraquark state of $I^GJ^{PC} = 0^+1^{-+}$ [95,96]. Based on this interpretation, one naturally expects the existence of the $ss\bar{s}\bar{s}$ tetraquark state with $I^GJ^{PC} = 0^+1^{-+}$, which we shall pay special attention to in the present study.

This paper is organized as follows. In Sec. II, we systematically construct the S- and P-wave fully strange tetraquark states as well as their corresponding interpolating currents. We use these currents to perform QCD sum rule analyses in Sec. III, and the obtained results are summarized and discussed in Sec. IV.

II. PHENOMENOLOGICAL ANALYSES

In this section we follow Ref. [38] to construct the S- and P-wave fully strange tetraquark states. We shall also construct their corresponding fully strange tetraquark currents by explicitly adding the covariant derivative operator $D_\alpha = \partial_\alpha + ig_sA_\alpha$, so that these currents behave well under the Lorentz transformation. We shall work within the diquark-antidiquark picture in the present study.

To start with, we investigate the ss diquark composed of two identical strange quarks with the *symmetric* flavor structure. According to the Pauli principle, the two strange quarks should be totally *antisymmetric*. As depicted in Fig. 2, we can construct two S-wave ss diquarks with the *symmetric* orbital structure:

(i) We use ${}^{2s+1}l_j = {}^3S_1$ to denote the S-wave ss diquark of $j^P = 1^+$ and the color representation $\bar{\mathbf{3}}_c$, where s, l, and j are its spin, orbital, and total angular momenta, respectively. The corresponding antidiquark is denoted as ${}^{2\bar{s}+1}\bar{l}_{\bar{j}} = {}^{\bar{3}}\bar{S}_{\bar{1}}$, where $\bar{s}$, $\bar{l}$, and $\bar{j}$ are its spin, orbital, and total angular momenta, respectively. This ${}^3S_1$ diquark has the *symmetric* spin and *antisymmetric* color structures, and its corresponding diquark field is

$$s_a^T C\gamma_\mu s_b, \tag{1}$$

where a and b are color indices, $C = i\gamma_2\gamma_0$ is the charge-conjugation operator, and the sum over repeated indices is taken. The superscript T represents the transpose of the Dirac index only, while the color index is not transposed.

(ii) We use ${}^1S_0$ to denote the S-wave ss diquark of $j^P = 0^+$ and the color representation $\mathbf{6}_c$. It has the *antisymmetric* spin and *symmetric* color structures, and its corresponding diquark field is

$$s_a^T C\gamma_5 s_b. \tag{2}$$

As depicted in Fig. 2, we can construct four P-wave ss diquarks with the *antisymmetric* orbital structure:

(i) We use ${}^1P_1$ to denote the P-wave ss diquark having $s = 0$, $j^P = 1^-$, and the color representation $\bar{\mathbf{3}}_c$. It has the *antisymmetric* spin and *antisymmetric* color structures, and its corresponding diquark field is

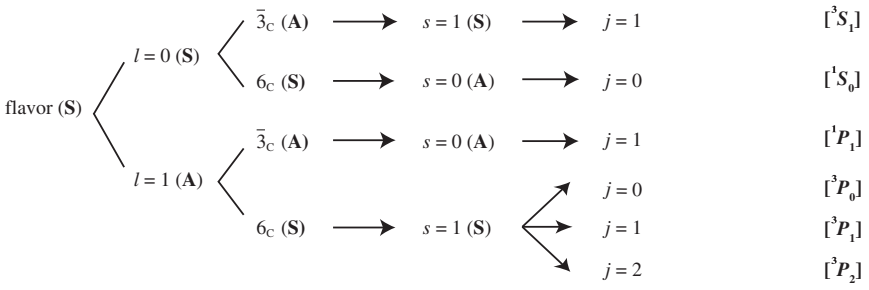

(a)

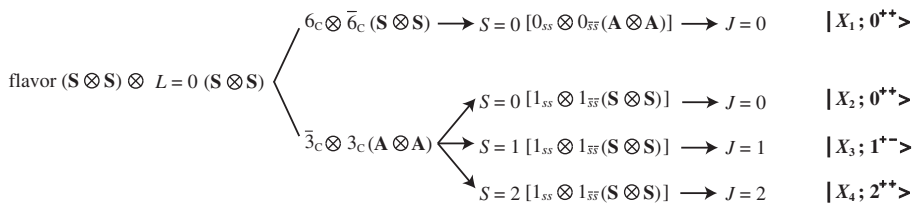

(b)

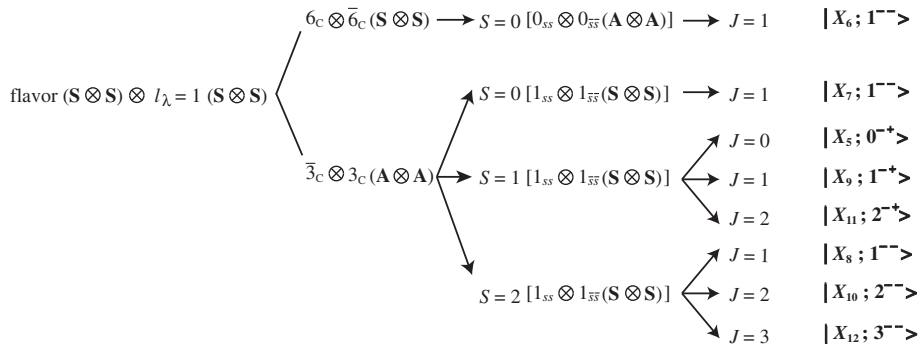

(c)

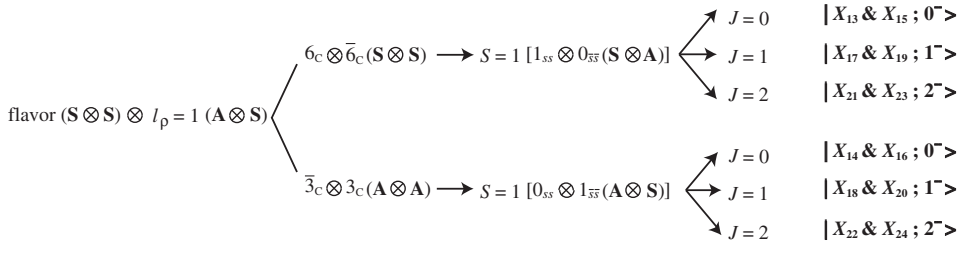

(d)

FIG. 2. Categorization of the S- and P-wave ss diquarks as well as the S- and P-wave $ss\bar{s}\bar{s}$ tetraquark states. One needs to further reorganize the S- and P-wave diquarks/antidiquarks in order to obtain the two states $|X_{13}; J^{PC} = 0^{--}\rangle$ and $|X_{15}; J^{PC} = 0^{-+}\rangle$, as well as all the other P-wave $ss\bar{s}\bar{s}$ tetraquark states of the ρ-mode. (a) S- and P-wave ss diquarks (b) S-wave $[ss][\bar{s}\bar{s}]$ tetraquark states (c) P-wave $[ss][\bar{s}\bar{s}]$ tetraquark states of the λ-mode (d) P-wave $[ss][\bar{s}\bar{s}]$ tetraquark states of the ρ-mode.

$$[s_a^T C\gamma_5 \overleftrightarrow{D}_\mu s_b], \tag{3}$$

with $[X\overleftrightarrow{D}_\mu Y] = X[D_\mu Y] - [D_\mu X]Y$. Note that the operator D_α carries color indices, e.g.,

$$\begin{aligned} D_\alpha s_a &= \partial_\alpha s_a + ig_s A_\alpha s_a \\ &= \partial_\alpha s_a + ig_s A_\alpha^n \frac{\lambda_{ab}^n}{2} s_b. \end{aligned} \tag{4}$$

For simplicity, we shall still use the notation $D_\alpha s_a$ so that $D_\alpha[s_a^T C\gamma_\mu s_b] = [D_\alpha s_a]^T C\gamma_\mu s_b + s_a^T C\gamma_\mu [D_\alpha s_b]$.

(ii) We use $^3P_0$ to denote the P-wave ss diquark having $s=1$, $j^P=0^-$, and the color representation $\mathbf{6}_c$. It has the *symmetric* spin and *symmetric* color structures, and its corresponding diquark field is

$$[s_a^T C\gamma^\mu \overleftrightarrow{D}_\mu s_b]. \tag{5}$$

(iii) We use $^3P_1$ to denote the P-wave ss diquark having $s=1$, $j^P=1^-$, and the color representation $\mathbf{6}_c$. It has the *symmetric* spin and *symmetric* color structures, and its corresponding diquark field is

$$[s_a^T C\gamma_\mu \overleftrightarrow{D}_\nu s_b]-\{\mu\leftrightarrow\nu\}. \tag{6}$$

(iv) We use $^3P_2$ to denote the P-wave ss diquark having $s=1$, $j^P=2^-$, and the color representation $\mathbf{6}_c$. It has the *symmetric* spin and *symmetric* color structures, and its corresponding diquark field is

$$\mathcal{S}[s_a^T C\gamma_\mu \overleftrightarrow{D}_\nu s_b], \tag{7}$$

where $\mathcal{S}$ denotes symmetrization and subtracting the trace term in the set $\{\mu\nu\}$.

In the following subsections we shall use the above S- and P-wave ss diquarks/antidiquarks to systematically construct the S- and P-wave $ss\bar{s}\bar{s}$ tetraquark states as well as their corresponding interpolating currents. Their color structure can be either

$$\bar{\mathbf{3}}_{ss}\otimes\mathbf{3}_{\bar{s}\bar{s}}\to\mathbf{1}_{[ss][\bar{s}\bar{s}]} \tag{8}$$

or

$$\mathbf{6}_{ss}\otimes\bar{\mathbf{6}}_{\bar{s}\bar{s}}\to\mathbf{1}_{[ss][\bar{s}\bar{s}]}. \tag{9}$$

A. S-wave states

In this subsection we use the S-wave ss diquarks/antidiquarks to construct the S-wave $ss\bar{s}\bar{s}$ tetraquark states. We denote them as $|X;J^{PC}\rangle=|^{2s+1}l_j,{}^{2\bar{s}+1}\bar{l}_{\bar{j}};J\rangle$.

As depicted in Fig. 2, we can construct four S-wave $ss\bar{s}\bar{s}$ tetraquark states:

$$\begin{aligned}
|X_1;0^{++}\rangle&=|^1S_0,{}^{\bar{1}}\bar{S}_{\bar{0}};J=0\rangle,\\
|X_2;0^{++}\rangle&=|^3S_1,{}^{\bar{3}}\bar{S}_{\bar{1}};J=0\rangle,\\
|X_3;1^{+-}\rangle&=|^3S_1,{}^{\bar{3}}\bar{S}_{\bar{1}};J=1\rangle,\\
|X_4;2^{++}\rangle&=|^3S_1,{}^{\bar{3}}\bar{S}_{\bar{1}};J=2\rangle.
\end{aligned} \tag{10}$$

Their corresponding interpolating currents are

$$J_1^{0^{++}}=s_a^T C\gamma_5 s_b\bar{s}_a\gamma_5 C\bar{s}_b^T, \tag{11}$$

$$J_2^{0^{++}}=s_a^T C\gamma_\mu s_b\bar{s}_a\gamma^\mu C\bar{s}_b^T, \tag{12}$$

$$\begin{aligned}
J_{3,\alpha}^{1^{+-}}&=s_a^T C\gamma^\mu s_b\bar{s}_a\sigma_{\alpha\mu}\gamma_5 C\bar{s}_b^T\\
&\quad-s_a^T C\sigma_{\alpha\mu}\gamma_5 s_b\bar{s}_a\gamma^\mu C\bar{s}_b^T,
\end{aligned} \tag{13}$$

$$J_{4,\alpha_1\alpha_2}^{2^{++}}=g_{\alpha_1\mu}g_{\alpha_2\nu}\mathcal{S}[s_a^T C\gamma^\mu s_b\bar{s}_a\gamma^\nu C\bar{s}_b^T]. \tag{14}$$

We have used the tensor diquark field $s_a^T C\sigma_{\mu\nu}\gamma_5 s_b$ to construct the third current $J_{3,\alpha}^{1^{+-}}$. In principle, this tensor diquark field can couple to both the $j^P=1^+$ and 1^- channels, but its positive-parity component $s_a^T C\sigma_{ij}\gamma_5 s_b$ ($i,\ j=1,\ 2,\ 3$) gives the dominant contribution to $J_{3,i}^{1^{+-}}$ ($i=1,\ 2,\ 3$). Therefore, the tetraquark current $J_{3,\alpha}^{1^{+-}}$ corresponds to the state $|X_3;1^{+-}\rangle$.

B. P-wave states of the λ-mode

In this subsection we use the S-wave ss diquarks/antidiquarks to construct the P-wave $ss\bar{s}\bar{s}$ tetraquark states of the λ-mode. These states have the total orbital excitation $L=1$ with $l_\lambda=1$ and $l_\rho=0$, so we call them λ-mode excitations. We denote them as $|X;J^{PC}\rangle=|^{2s+1}l_j,{}^{2\bar{s}+1}\bar{l}_{\bar{j}};S,J,\lambda\rangle$.

As depicted in Fig. 2, we can construct eight P-wave $ss\bar{s}\bar{s}$ states of the λ-mode:

$$\begin{aligned}
|X_5;0^{-+}\rangle&=|^3S_1,{}^{\bar{3}}\bar{S}_{\bar{1}};S=1,J=0,\lambda\rangle,\\
|X_6;1^{--}\rangle&=|^1S_0,{}^{\bar{1}}\bar{S}_{\bar{0}};S=0,J=1,\lambda\rangle,\\
|X_7;1^{--}\rangle&=|^3S_1,{}^{\bar{3}}\bar{S}_{\bar{1}};S=0,J=1,\lambda\rangle,\\
|X_8;1^{--}\rangle&=|^3S_1,{}^{\bar{3}}\bar{S}_{\bar{1}};S=2,J=1,\lambda\rangle,\\
|X_9;1^{-+}\rangle&=|^3S_1,{}^{\bar{3}}\bar{S}_{\bar{1}};S=1,J=1,\lambda\rangle,\\
|X_{10};2^{--}\rangle&=|^3S_1,{}^{\bar{3}}\bar{S}_{\bar{1}};S=2,J=2,\lambda\rangle,\\
|X_{11};2^{-+}\rangle&=|^3S_1,{}^{\bar{3}}\bar{S}_{\bar{1}};S=1,J=2,\lambda\rangle,\\
|X_{12};3^{--}\rangle&=|^3S_1,{}^{\bar{3}}\bar{S}_{\bar{1}};S=2,J=3,\lambda\rangle.
\end{aligned} \tag{15}$$

Their corresponding interpolating currents are

$$\begin{aligned}
J_5^{0^{-+}}&=[s_a^T C\gamma^\nu s_b]\overleftrightarrow{D}^\mu[\bar{s}_a\sigma_{\mu\nu}\gamma_5 C\bar{s}_b^T]\\
&\quad-[s_a^T C\sigma_{\mu\nu}\gamma_5 s_b]\overleftrightarrow{D}^\mu[\bar{s}_a\gamma^\nu C\bar{s}_b^T],
\end{aligned} \tag{16}$$

$$J_{6,\alpha}^{1^{--}}=[s_a^T C\gamma_5 s_b]\overleftrightarrow{D}_\alpha[\bar{s}_a\gamma_5 C\bar{s}_b^T], \tag{17}$$

$$J_{7,\alpha}^{1^{--}}=[s_a^T C\gamma_\mu s_b]\overleftrightarrow{D}_\alpha[\bar{s}_a\gamma^\mu C\bar{s}_b^T], \tag{18}$$

$$J_{8,\alpha}^{1^{--}}=g_{\alpha\mu}g_{\nu\rho}\mathcal{S}[[s_a^T C\gamma^\mu s_b]\overleftrightarrow{D}^\rho[\bar{s}_a\gamma^\nu C\bar{s}_b^T]], \tag{19}$$

$$J^{1^{-+}}_{9,\alpha} = [s_a^T C\gamma_\alpha s_b]\overleftrightarrow{D}^\mu[\bar{s}_a\gamma_\mu C\bar{s}_b^T] - [s_a^T C\gamma_\mu s_b]\overleftrightarrow{D}^\mu[\bar{s}_a\gamma_\alpha C\bar{s}_b^T], \tag{20}$$

$$J^{2^{--}}_{10,\alpha_1\alpha_2} = g_{\alpha_1\mu}g_{\alpha_2\nu}\mathcal{S}[[s_a^T C\gamma^\mu s_b]\overleftrightarrow{D}_\rho[\bar{s}_a\sigma^{\nu\rho}\gamma_5 C\bar{s}_b^T] + [s_a^T C\sigma^{\nu\rho}\gamma_5 s_b]\overleftrightarrow{D}_\rho[\bar{s}_a\gamma^\mu C\bar{s}_b^T]], \tag{21}$$

$$J^{2^{-+}}_{11,\alpha_1\alpha_2} = g_{\alpha_1\mu}g_{\alpha_2\nu}\mathcal{S}[[s_a^T C\gamma_\rho s_b]\overleftrightarrow{D}^\mu[\bar{s}_a\sigma^{\nu\rho}\gamma_5 C\bar{s}_b^T] - [s_a^T C\sigma^{\nu\rho}\gamma_5 s_b]\overleftrightarrow{D}^\mu[\bar{s}_a\gamma_\rho C\bar{s}_b^T]], \tag{22}$$

$$J^{3^{--}}_{12,\alpha_1\alpha_2\alpha_3} = \mathcal{S}'[[s_a^T C\gamma_{\alpha_1} s_b]\overleftrightarrow{D}_{\alpha_2}[\bar{s}_a\gamma_{\alpha_3} C\bar{s}_b^T]], \tag{23}$$

where $\mathcal{S}'$ denotes symmetrization and subtracting trace terms in the set $\{\alpha_1\alpha_2\alpha_3\}$.

C. P-wave states of the ρ-mode

In this subsection we use the S- and P-wave ss diquarks/antidiquarks to construct the P-wave $ss\bar{s}\bar{s}$ tetraquark states of the ρ-mode. These states have the total orbital excitation $L = 1$ with $l_\lambda = 0$ and $l_\rho = 1$, so we call them ρ-mode excitations. We denote them as $|X; J^{PC}\rangle = |^{2s+1}l_j, {}^{2\bar{s}+1}\bar{l}_{\bar{j}}; S, J, \rho\rangle$.

As depicted in Fig. 2, we can construct 12 P-wave $ss\bar{s}\bar{s}$ states of the ρ-mode:

$$\begin{aligned}
|X_{13}; 0^{--}\rangle &= |^1S_0, {}^{\bar{3}}\bar{P}_{\bar{0}}; 1, 0, \rho\rangle - |^3P_0, {}^{\bar{1}}\bar{S}_{\bar{0}}; 1, 0, \rho\rangle,\\
|X_{14}; 0^{--}\rangle &= |^3S_1, {}^{\bar{1}}\bar{P}_{\bar{1}}; 1, 0, \rho\rangle - |^1P_1, {}^{\bar{3}}\bar{S}_{\bar{1}}; 1, 0, \rho\rangle,\\
|X_{15}; 0^{-+}\rangle &= |^1S_0, {}^{\bar{3}}\bar{P}_{\bar{0}}; 1, 0, \rho\rangle + |^3P_0, {}^{\bar{1}}\bar{S}_{\bar{0}}; 1, 0, \rho\rangle,\\
|X_{16}; 0^{-+}\rangle &= |^3S_1, {}^{\bar{1}}\bar{P}_{\bar{1}}; 1, 0, \rho\rangle + |^1P_1, {}^{\bar{3}}\bar{S}_{\bar{1}}; 1, 0, \rho\rangle,\\
|X_{17}; 1^{--}\rangle &= |^1S_0, {}^{\bar{3}}\bar{P}_{\bar{1}}; 1, 1, \rho\rangle - |^3P_1, {}^{\bar{1}}\bar{S}_{\bar{0}}; 1, 1, \rho\rangle,\\
|X_{18}; 1^{--}\rangle &= |^3S_1, {}^{\bar{1}}\bar{P}_{\bar{1}}; 1, 1, \rho\rangle - |^1P_1, {}^{\bar{3}}\bar{S}_{\bar{1}}; 1, 1, \rho\rangle,\\
|X_{19}; 1^{-+}\rangle &= |^1S_0, {}^{\bar{3}}\bar{P}_{\bar{1}}; 1, 1, \rho\rangle + |^3P_1, {}^{\bar{1}}\bar{S}_{\bar{0}}; 1, 1, \rho\rangle,\\
|X_{20}; 1^{-+}\rangle &= |^3S_1, {}^{\bar{1}}\bar{P}_{\bar{1}}; 1, 1, \rho\rangle + |^1P_1, {}^{\bar{3}}\bar{S}_{\bar{1}}; 1, 1, \rho\rangle,\\
|X_{21}; 2^{--}\rangle &= |^1S_0, {}^{\bar{3}}\bar{P}_{\bar{2}}; 1, 2, \rho\rangle - |^3P_2, {}^{\bar{1}}\bar{S}_{\bar{0}}; 1, 2, \rho\rangle,\\
|X_{22}; 2^{--}\rangle &= |^3S_1, {}^{\bar{1}}\bar{P}_{\bar{1}}; 1, 2, \rho\rangle - |^1P_1, {}^{\bar{3}}\bar{S}_{\bar{1}}; 1, 2, \rho\rangle,\\
|X_{23}; 2^{-+}\rangle &= |^1S_0, {}^{\bar{3}}\bar{P}_{\bar{2}}; 1, 2, \rho\rangle + |^3P_2, {}^{\bar{1}}\bar{S}_{\bar{0}}; 1, 2, \rho\rangle,\\
|X_{24}; 2^{-+}\rangle &= |^3S_1, {}^{\bar{1}}\bar{P}_{\bar{1}}; 1, 2, \rho\rangle + |^1P_1, {}^{\bar{3}}\bar{S}_{\bar{1}}; 1, 2, \rho\rangle.
\end{aligned} \tag{24}$$

Their corresponding interpolating currents are

$$J^{0^{--}}_{13} = [s_a^T C\gamma_5 s_b][\bar{s}_a\gamma^\mu C\overleftrightarrow{D}_\mu\bar{s}_b^T] - [s_a^T C\gamma^\mu\overleftrightarrow{D}_\mu s_b][\bar{s}_a\gamma_5 C\bar{s}_b^T], \tag{25}$$

$$J^{0^{--}}_{14} = [s_a^T C\gamma^\mu s_b][\bar{s}_a\gamma_5 C\overleftrightarrow{D}_\mu\bar{s}_b^T] - [s_a^T C\gamma_5\overleftrightarrow{D}_\mu s_b][\bar{s}_a\gamma^\mu C\bar{s}_b^T], \tag{26}$$

$$J^{0^{-+}}_{15} = [s_a^T C\gamma_5 s_b][\bar{s}_a\gamma^\mu C\overleftrightarrow{D}_\mu\bar{s}_b^T] + [s_a^T C\gamma^\mu\overleftrightarrow{D}_\mu s_b][\bar{s}_a\gamma_5 C\bar{s}_b^T], \tag{27}$$

$$J^{0^{-+}}_{16} = [s_a^T C\gamma^\mu s_b][\bar{s}_a\gamma_5 C\overleftrightarrow{D}_\mu\bar{s}_b^T] + [s_a^T C\gamma_5\overleftrightarrow{D}_\mu s_b][\bar{s}_a\gamma^\mu C\bar{s}_b^T], \tag{28}$$

$$J^{1^{--}}_{17,\alpha\beta} = [s_a^T C\gamma_5 s_b][\bar{s}_a\gamma_\beta C\overleftrightarrow{D}_\alpha\bar{s}_b^T] - [s_a^T C\gamma_\beta\overleftrightarrow{D}_\alpha s_b][\bar{s}_a\gamma_5 C\bar{s}_b^T] - \{\alpha\leftrightarrow\beta\}, \tag{29}$$

$$J^{1^{--}}_{18,\alpha\beta} = [s_a^T C\gamma_\beta s_b][\bar{s}_a\gamma_5 C\overleftrightarrow{D}_\alpha\bar{s}_b^T] - [s_a^T C\gamma_5\overleftrightarrow{D}_\alpha s_b][\bar{s}_a\gamma_\beta C\bar{s}_b^T] - \{\alpha\leftrightarrow\beta\}, \tag{30}$$

$$J^{1^{-+}}_{19,\alpha\beta} = [s_a^T C\gamma_5 s_b][\bar{s}_a\gamma_\beta C\overleftrightarrow{D}_\alpha\bar{s}_b^T] + [s_a^T C\gamma_\beta\overleftrightarrow{D}_\alpha s_b][\bar{s}_a\gamma_5 C\bar{s}_b^T] - \{\alpha\leftrightarrow\beta\}, \tag{31}$$

$$J^{1^{-+}}_{20,\alpha\beta} = [s_a^T C\gamma_\beta s_b][\bar{s}_a\gamma_5 C\overleftrightarrow{D}_\alpha\bar{s}_b^T] + [s_a^T C\gamma_5\overleftrightarrow{D}_\alpha s_b][\bar{s}_a\gamma_\beta C\bar{s}_b^T] - \{\alpha\leftrightarrow\beta\}, \tag{32}$$

$$J^{2^{--}}_{21,\alpha_1\alpha_2} = g_{\alpha_1\mu}g_{\alpha_2\nu}\mathcal{S}[[s_a^T C\gamma_5 s_b][\bar{s}_a\gamma^\nu C\overleftrightarrow{D}^\mu\bar{s}_b^T] - [s_a^T C\gamma^\nu\overleftrightarrow{D}^\mu s_b][\bar{s}_a\gamma_5 C\bar{s}_b^T]], \tag{33}$$

$$J^{2^{--}}_{22,\alpha_1\alpha_2} = g_{\alpha_1\mu}g_{\alpha_2\nu}\mathcal{S}[[s_a^T C\gamma^\nu s_b][\bar{s}_a\gamma_5 C\overleftrightarrow{D}^\mu\bar{s}_b^T] - [s_a^T C\gamma_5\overleftrightarrow{D}^\mu s_b][\bar{s}_a\gamma^\nu C\bar{s}_b^T]], \tag{34}$$

$$J^{2^{-+}}_{23,\alpha_1\alpha_2} = g_{\alpha_1\mu}g_{\alpha_2\nu}\mathcal{S}[[s_a^T C\gamma_5 s_b][\bar{s}_a\gamma^\nu C\overleftrightarrow{D}^\mu\bar{s}_b^T] + [s_a^T C\gamma^\nu\overleftrightarrow{D}^\mu s_b][\bar{s}_a\gamma_5 C\bar{s}_b^T]], \tag{35}$$

$$J^{2^{-+}}_{24,\alpha_1\alpha_2} = g_{\alpha_1\mu}g_{\alpha_2\nu}\mathcal{S}[[s_a^T C\gamma^\nu s_b][\bar{s}_a\gamma_5 C\overleftrightarrow{D}^\mu\bar{s}_b^T] + [s_a^T C\gamma_5\overleftrightarrow{D}^\mu s_b][\bar{s}_a\gamma^\nu C\bar{s}_b^T]]. \tag{36}$$

The four currents $J^{\cdots}_{17\cdots20,\alpha\beta}$ all have two antisymmetric Lorentz indices α and β, so they actually contain both $J^P = 1^-$ and 1^+ components. In the present study we shall

use these currents to study the four $J^P = 1^-$ states $|X_{17\cdots20}; 1^{-\pm}\rangle$ through

$$\langle 0|J^{\cdots}_{17\cdots20,\alpha\beta}|X_{17\cdots20}(\epsilon,q)\rangle = if_{X_{17\cdots20}}\boldsymbol{\epsilon}_{\alpha\beta\rho\sigma}\epsilon^{\rho}q^{\sigma}, \quad (37)$$

where ϵ^{ρ} is the polarization vector, $\boldsymbol{\epsilon}_{\alpha\beta\rho\sigma}$ is the totally antisymmetric tensor, and $f_{X_{17\cdots20}}$ are the decay constants. Note that these four currents can also couple to the four $J^P = 1^+$ states $|X'_{17\cdots20}; 1^{+\pm}\rangle$ through

$$\langle 0|J^{\cdots}_{17\cdots20,\alpha\beta}|X'_{17\cdots20}(\epsilon,q)\rangle = if_{X'_{17\cdots20}}(q_{\alpha}\epsilon_{\beta} - q_{\beta}\epsilon_{\alpha}). \quad (38)$$

Technically, we can easily isolate $|X_{17\cdots20}; 1^{-\pm}\rangle$ at the hadron level by investigating the correlation function proportional to

$$\begin{aligned}&\langle 0|J^{\cdots}_{17\cdots20,\alpha\beta}|X_{17\cdots20}\rangle\langle X_{17\cdots20}|J^{\cdots,\dagger}_{17\cdots20,\alpha'\beta'}|0\rangle\\ &= f^2_{X_{17\cdots20}}\boldsymbol{\epsilon}_{\alpha\beta\rho\sigma}\epsilon^{\rho}q^{\sigma}\boldsymbol{\epsilon}_{\alpha'\beta'\rho'\sigma'}\epsilon^{*\rho'}q^{\sigma'}\\ &= -f^2_{X_{17\cdots20}}q^2(g_{\alpha\alpha'}g_{\beta\beta'} - g_{\alpha\beta'}g_{\beta\alpha'}) + \cdots, \end{aligned} \quad (39)$$

given that the correlation function of $|X'_{17\cdots20}; 1^{+\pm}\rangle$ does not contain the above coefficient.

III. QCD SUM RULE ANALYSIS

The method of QCD sum rules is a powerful and successful nonperturbative method [97–103]. In this section we apply this method to study the 24 currents given in Eqs. (11)–(14), Eqs. (16)–(23), and Eqs. (25)–(36).

The four currents $J^{\cdots}_{17\cdots20,\alpha\beta}$ couple to the states $|X_{17\cdots20}; J^{PC}\rangle$ through Eq. (37). The other 20 currents $J^{\cdots}_{1\cdots16/21\ldots24,\alpha_1\cdots\alpha_J}$ of spin-J couple to the states $|X_{1\cdots16/21\ldots24}; J^{PC}\rangle$ through

$$\begin{aligned}&\langle 0|J^{\cdots}_{1\cdots16/21\ldots24,\alpha_1\cdots\alpha_J}|X_{1\cdots16/21\ldots24}; J^{PC}\rangle\\ &= f_{X_{1\cdots16/21\ldots24}}\epsilon_{\alpha_1\cdots\alpha_J}. \end{aligned} \quad (40)$$

Here f_X is the decay constant, and $\epsilon_{\alpha_1\cdots\alpha_J}$ is the traceless and symmetric polarization tensor, satisfying

$$\epsilon_{\alpha_1\cdots\alpha_J}\epsilon^*_{\beta_1\cdots\beta_J} = \mathcal{S}''[\tilde{g}_{\alpha_1\beta_1}\cdots\tilde{g}_{\alpha_J\beta_J}], \quad (41)$$

where $\tilde{g}_{\mu\nu} = g_{\mu\nu} - q_{\mu}q_{\nu}/q^2$ and $\mathcal{S}''$ denotes symmetrization and subtracting trace terms in the sets $\{\alpha_1\cdots\alpha_J\}$ and $\{\beta_1\cdots\beta_J\}$.

We use the current $J_1^{0^{++}}$ as an example and study its two-point correlation function

$$\Pi(q^2) = i\int d^4x e^{iqx}\langle 0|\mathbf{T}[J_1^{0^{++}}(x)J_1^{0^{++},\dagger}(0)]|0\rangle, \quad (42)$$

at both the hadron and the quark-gluon levels.

At the hadron level we express Eq. (42) through the dispersion relation as

$$\Pi(q^2) = \int_{16m_s^2}^{\infty}\frac{\rho(s)}{s - q^2 - i\varepsilon}ds, \quad (43)$$

where $\rho(s) \equiv \mathrm{Im}\Pi(s)/\pi$ is the spectral density. We parametrize it as one pole dominance for the ground state $|X_1; 0^{++}\rangle$ and a continuum contribution:

$$\begin{aligned}\rho_{\mathrm{phen}}(s) &\equiv \sum_n \delta(s - M_n^2)\langle 0|J_1^{0^{++}}|n\rangle\langle n|J_1^{0^{++},\dagger}|0\rangle\\ &= f_X^2\delta(s - M_X^2) + \text{continuum}. \end{aligned} \quad (44)$$

At the quark-gluon level we apply the method of operator product expansion (OPE) to calculate Eq. (42) and extract the OPE spectral density $\rho_{\mathrm{OPE}}(s)$. After performing the Borel transformation at both the hadron and quark-gluon levels, we approximate the continuum using $\rho_{\mathrm{OPE}}(s)$ above a threshold value s_0 and arrive at the sum rule equation

$$\Pi(s_0, M_B^2) \equiv f_X^2 e^{-M_X^2/M_B^2} = \int_{16m_s^2}^{s_0} e^{-s/M_B^2}\rho_{\mathrm{OPE}}(s)ds, \quad (45)$$

which can be used to calculate M_X through

$$M_X^2(s_0, M_B) = \frac{\int_{16m_s^2}^{s_0} e^{-s/M_B^2}s\rho_{\mathrm{OPE}}(s)ds}{\int_{16m_s^2}^{s_0} e^{-s/M_B^2}\rho_{\mathrm{OPE}}(s)ds}. \quad (46)$$

In this study we take into account the Feynman diagrams depicted in Fig. 3. The covariant derivative operator $D_{\alpha} = \partial_{\alpha} + ig_sA_{\alpha}$ can be naturally separated into two parts, and we depict the latter term using a green vertex; e.g., see the diagrams depicted in Figs. 3(d)–3(i) and Figs. 3(g)–3(i). In the calculations we have taken into account the perturbative term, the strange quark mass m_s, the quark condensate $\langle\bar{s}s\rangle$, the gluon condensate $\langle g_s^2GG\rangle$, the quark-gluon mixed condensate $\langle g_s\bar{s}\sigma Gs\rangle$, and their combinations. We have assumed the vacuum saturation for higher dimensional operators, e.g., $\langle\bar{s}s\bar{s}s\rangle \approx \langle\bar{s}s\rangle^2$ and $\langle\bar{s}sg_s\bar{s}\sigma Gs\rangle \approx \langle\bar{s}s\rangle\langle g_s\bar{s}\sigma Gs\rangle$. Other condensates such as $\langle g_s^3G^3\rangle$ and $\langle g_s\bar{s}D_{\mu}G^{\mu\nu}\gamma_{\nu}s\rangle$ are not considered in the present study. We have taken into account all the diagrams proportional to $g_s^{N=0}$ and $g_s^{N=1}$. We find that the $D = 6$ term $\langle\bar{s}s\rangle^2$ and the $D = 8$ term $\langle\bar{s}s\rangle\langle g_s\bar{s}\sigma Gs\rangle$ are important. We have only partly calculated the diagrams proportional to $g_s^{N\geq2}$, whose contributions are found to be small.

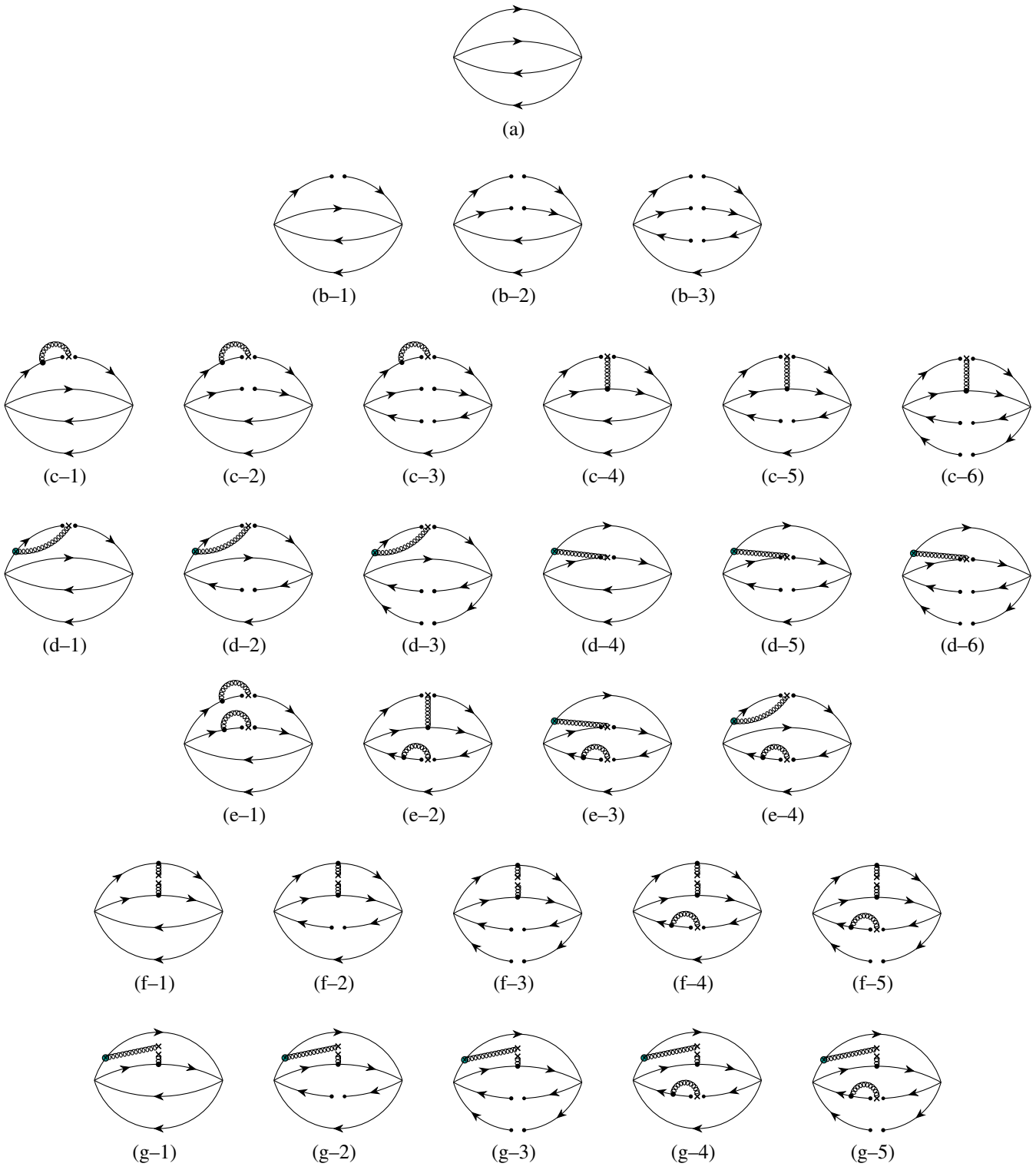

FIG. 3. Feynman diagrams for the fully strange tetraquark states, including the perturbative term, the strange quark mass m_s, the quark condensate $\langle \bar{s}s \rangle$, the gluon condensate $\langle g_s^2 GG \rangle$, the quark-gluon mixed condensate $\langle \bar{g}_s s\sigma Gs \rangle$, and their combinations. Diagrams (a) and (b)–(i) are proportional to $g_s^{N=0}$; diagrams (c)–(i) and (d)–(i) are proportional to $g_s^{N=1}$; diagrams (e)–(i), (f)–(i), and (g)–(i) are proportional to $g_s^{N\geq 2}$.

The sum rule equation from the current J_1^{0++} is

$$\Pi_{11} = \int_{16m_s^2}^{s_0} e^{-s/M^2} ds \times \left[\frac{s^4}{30720\pi^6} - \frac{m_s^2 s^3}{768\pi^6} + \left(-\frac{\langle g_s^2 GG\rangle}{6144\pi^6} - \frac{m_s\langle \bar{s}s\rangle}{48\pi^4}\right)s^2 + \left(\frac{\langle \bar{s}s\rangle^2}{6\pi^2} - \frac{m_s\langle g_s\bar{s}\sigma Gs\rangle}{16\pi^4} + \frac{\langle g_s^2 GG\rangle m_s^2}{1024\pi^6}\right)s + \frac{\langle \bar{s}s\rangle\langle g_s\bar{s}\sigma Gs\rangle}{6\pi^2} + \frac{\langle g_s^2 GG\rangle m_s\langle \bar{s}s\rangle}{384\pi^4} - \frac{m_s^2\langle \bar{s}s\rangle^2}{12\pi^2}\right] + \left(\frac{\langle g_s\bar{s}\sigma Gs\rangle^2}{48\pi^2} - \frac{\langle g_s^2 GG\rangle\langle \bar{s}s\rangle^2}{288\pi^2} + \frac{\langle g_s^2 GG\rangle m_s\langle g_s\bar{s}\sigma Gs\rangle}{768\pi^4} - \frac{4m_s\langle \bar{s}s\rangle^3}{9}\right) + \frac{1}{M_B^2}\left(\frac{\langle g_s^2 GG\rangle\langle \bar{s}s\rangle\langle g_s\bar{s}\sigma Gs\rangle}{576\pi^2} + \frac{\langle g_s^2 GG\rangle m_s^2\langle \bar{s}s\rangle^2}{1152\pi^2} - \frac{m_s^2\langle g_s\bar{s}\sigma Gs\rangle^2}{48\pi^2} + \frac{4m_s\langle \bar{s}s\rangle^2\langle g_s\bar{s}\sigma Gs\rangle}{9}\right). \quad (47)$$

Sum rule equations extracted from other currents are given in the Appendix, which will be used to perform numerical analyses using the following values for various QCD parameters [1,104–110]:

$$\begin{aligned} m_s(2\text{ GeV}) &= 93^{+11}_{-5}\text{ MeV},\\ \langle g_s^2 GG\rangle &= (0.48\pm 0.14)\text{ GeV}^4,\\ \langle \bar{q}q\rangle &= -(0.240\pm 0.010)^3\text{ GeV}^3,\\ \langle \bar{s}s\rangle &= (0.8\pm 0.1)\times\langle \bar{q}q\rangle,\\ \langle g_s\bar{s}\sigma Gs\rangle &= -M_0^2\times\langle \bar{s}s\rangle,\\ M_0^2 &= (0.8\pm 0.2)\text{ GeV}^2. \end{aligned} \quad (48)$$

We use the spectral density given in Eq. (47) as an example to perform numerical analyses. It is extracted from the current J_1^{0++} and corresponds to the state $|X_1;0^{++}\rangle = |^1S_0,^{\bar{1}}\bar{S}_{\bar{0}};J=0\rangle$. As shown in Eq. (46), its mass M_X depends on two free parameters, the threshold value s_0, and the Borel mass M_B. We analyze three aspects to determine their working regions: (a) the convergence of OPE, (b) the pole contribution, and (c) the mass dependence on these two parameters.

First, we investigate the convergence of OPE and require the $D=12/10/8$ terms to be less than 5%/10%/20%, respectively:

$$\text{CVG}_{12} \equiv \left|\frac{\Pi_{11}^{D=12}(\infty,M_B^2)}{\Pi_{11}(\infty,M_B^2)}\right| \le 5\%, \quad (49)$$

$$\text{CVG}_{10} \equiv \left|\frac{\Pi_{11}^{D=10}(\infty,M_B^2)}{\Pi_{11}(\infty,M_B^2)}\right| \le 10\%, \quad (50)$$

$$\text{CVG}_{8} \equiv \left|\frac{\Pi_{11}^{D=8}(\infty,M_B^2)}{\Pi_{11}(\infty,M_B^2)}\right| \le 20\%. \quad (51)$$

This is the cornerstone of a reliable QCD sum rule analysis. As shown in Fig. 4 using three dashed curves, we determine the lower bound of the Borel mass to be $M_B^2 > 1.65\text{ GeV}^2$. Since we have only partly calculated the diagrams proportional to $g_s^{N\ge 2}$, it is useful to see how large these terms are

$$\left|\frac{\Pi_{11}^{g_s^{N=1}}(\infty,M_B^2)}{\Pi_{11}(\infty,M_B^2)}\right| \le 31.0\%, \quad (52)$$

$$\left|\frac{\Pi_{11}^{g_s^{N\ge 2}}(\infty,M_B^2)}{\Pi_{11}(\infty,M_B^2)}\right| \le 4.7\%. \quad (53)$$

Second, we investigate the one-pole-dominance assumption and require the pole contribution to be larger than 40%:

$$\text{Pole contribution} \equiv \left|\frac{\Pi_{11}(s_0,M_B^2)}{\Pi_{11}(\infty,M_B^2)}\right| \ge 40\%. \quad (54)$$

As shown in Fig. 4 using the solid curve, we determine the upper bound of the Borel mass to be $M_B^2 < 1.77\text{ GeV}^2$, when setting s_0 to be $s_0 = 6.5\text{ GeV}^2$. Altogether the Borel window is extracted to be $1.65\text{ GeV}^2 < M_B^2 < 1.77\text{ GeV}^2$ for $s_0 = 6.5\text{ GeV}^2$. We repeat the same procedures by

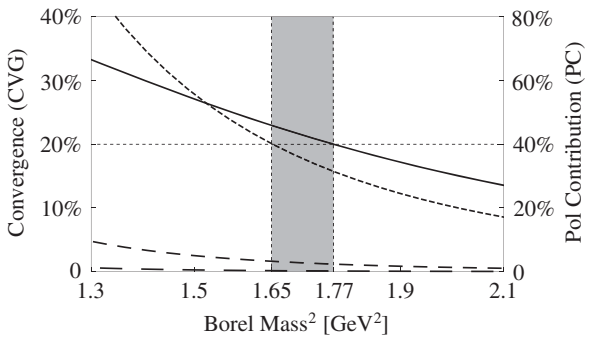

FIG. 4. CVG_{12} [long dashed curve defined in Eq. (49)], CVG_{10} [middle dashed curve defined in Eq. (50)], CVG_8 [short dashed curve defined in Eq. (51)], and the pole contribution [solid curve defined in Eq. (54)] as functions of the Borel mass M_B. These curves are obtained using the current J_1^{0++} with $s_0 = 6.5\text{ GeV}^2$.

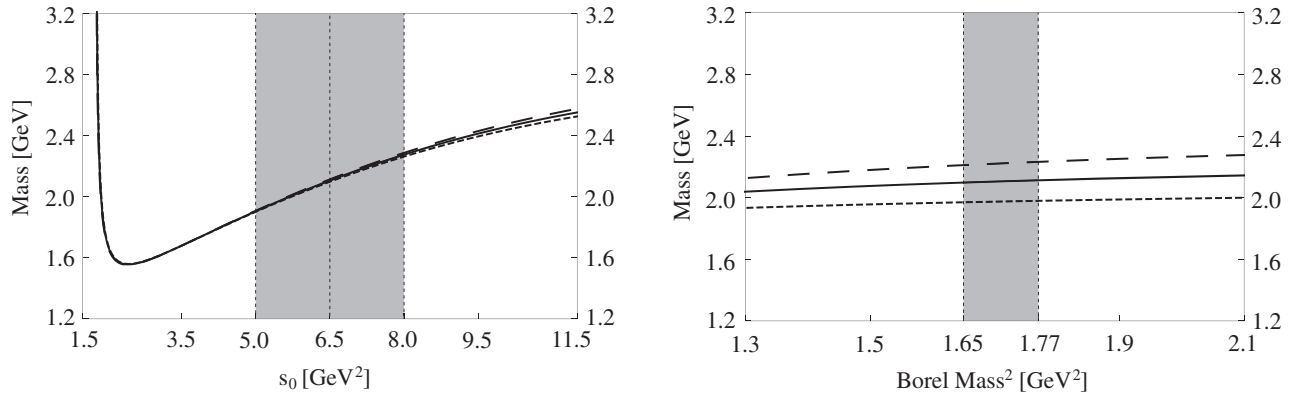

FIG. 5. Mass of $|X_1;0^{++}\rangle$ extracted from the current J_1^{0++}, as a function of the threshold value s_0 (left) and the Borel mass M_B (right). In the left panel the short-dashed/solid/long-dashed curves are plotted by setting $M_B^2 = 1.65/1.71/1.77$ GeV^2, respectively. In the right panel the short-dashed/solid/long-dashed curves are plotted by setting $s_0 = 5.5/6.5/7.5$ GeV^2, respectively.

changing s_0 and find that there are nonvanishing Borel windows as long as $s_0 > s_0^{\min} = 6.0$ GeV^2.

Third, we investigate the mass dependence on s_0 and M_B. We show M_X in Fig. 5 with respect to these two parameters. Its dependence on s_0 is moderate around $s_0 \sim 6.5$ GeV^2, and its dependence on M_B is weak inside the Borel window 1.65 GeV$^2 < M_B^2 < 1.77$ GeV^2. Accordingly, we choose the working regions of s_0 and M_B to be 5.0 GeV$^2 < s_0 <$ 8.0 GeV^2 and 1.65 GeV$^2 < M_B^2 < 1.77$ GeV^2, where the mass of $|X_1;0^{++}\rangle$ is evaluated to be

TABLE I. QCD sum rule results of the S- and P-wave fully strange tetraquark states, with possible experimental candidates given for comparisons.

Currents	Configuration	$s_0^{\min}$ [GeV^2]	Working regions		Pole [%]	Mass [GeV]	Candidate
			M_B^2 [GeV^2]	s_0 [GeV^2]			
J_1^{0++}	$\|X_1;0^{++}\rangle \sim \|^1S_0,^{\bar{1}}\bar{S}_{\bar{0}};J=0\rangle$	6.0	1.65–1.77	6.5 ± 1.5	40–46	$2.11^{+0.19}_{-0.21}$	$f_0(2100)$
J_2^{0++}	$\|X_2;0^{++}\rangle \sim \|^3S_1,^{\bar{3}}\bar{S}_{\bar{1}};J=0\rangle$	2.9	1.27–1.76	6.5 ± 1.5	40–70	$1.99^{+0.19}_{-0.24}$	…
J_3^{1+-}	$\|X_3;1^{+-}\rangle \sim \|^3S_1,^{\bar{3}}\bar{S}_{\bar{1}};J=1\rangle$	5.4	1.69–1.96	6.5 ± 1.5	40–53	$2.06^{+0.18}_{-0.20}$	$X(2063)$
J_4^{2++}	$\|X_4;2^{++}\rangle \sim \|^3S_1,^{\bar{3}}\bar{S}_{\bar{1}};J=2\rangle$	5.4	1.53–1.77	6.5 ± 1.5	40–53	$2.09^{+0.19}_{-0.22}$	$f_2(2010)$
J_5^{0-+}	$\|X_5;0^{-+}\rangle \sim \|^3S_1,^{\bar{3}}\bar{S}_{\bar{1}};1,0,\lambda\rangle$	3.5	1.48–1.99	8.5 ± 2.0	40–70	$2.31^{+0.21}_{-0.26}$	$X(2370)$
J_6^{1--}	$\|X_6;1^{--}\rangle \sim \|^1S_0,^{\bar{1}}\bar{S}_{\bar{0}};0,1,\lambda\rangle$	9.5	…	…	…	…	…
J_7^{1--}	$\|X_7;1^{--}\rangle \sim \|^3S_1,^{\bar{3}}\bar{S}_{\bar{1}};0,1,\lambda\rangle$	7.3	1.59–1.77	8.5 ± 2.0	40–52	$2.34^{+0.23}_{-0.30}$	$\phi(2170)$
J_8^{1--}	$\|X_8;1^{--}\rangle \sim \|^3S_1,^{\bar{3}}\bar{S}_{\bar{1}};2,1,\lambda\rangle$	10.1	…	…	…	…	…
J_9^{1-+}	$\|X_9;1^{-+}\rangle \sim \|^3S_1,^{\bar{3}}\bar{S}_{\bar{1}};1,1,\lambda\rangle$	10.5	…	…	…	…	…
J_{10}^{2--}	$\|X_{10};2^{--}\rangle \sim \|^3S_1,^{\bar{3}}\bar{S}_{\bar{1}};2,2,\lambda\rangle$	6.0	1.38–1.76	8.5 ± 2.0	40–66	$2.32^{+0.23}_{-0.30}$	…
J_{11}^{2-+}	$\|X_{11};2^{-+}\rangle \sim \|^3S_1,^{\bar{3}}\bar{S}_{\bar{1}};1,2,\lambda\rangle$	6.3	1.51–1.93	8.5 ± 2.0	40–64	$2.40^{+0.20}_{-0.25}$	…
J_{12}^{3--}	$\|X_{12};3^{--}\rangle \sim \|^3S_1,^{\bar{3}}\bar{S}_{\bar{1}};2,3,\lambda\rangle$	9.0	1.94–1.94	9.0 ± 2.0	40–40	$2.41^{+0.25}_{-0.30}$	…
J_{13}^{0--}	$\|X_{13};0^{--}\rangle \sim \|^1S_0,^{\bar{3}}\bar{P}_{\bar{0}};1,0,\rho\rangle$	11.5	…	…	…	…	…
J_{14}^{0--}	$\|X_{14};0^{--}\rangle \sim \|^3S_1,^{\bar{1}}\bar{P}_{\bar{1}};1,0,\rho\rangle$	7.4	1.51–1.74	8.5 ± 2.0	40–53	$2.50^{+0.21}_{-0.24}$	…
J_{15}^{0-+}	$\|X_{15};0^{-+}\rangle \sim \|^1S_0,^{\bar{3}}\bar{P}_{\bar{0}};1,0,\rho\rangle$	11.5	…	…	…	…	…
J_{16}^{0-+}	$\|X_{16};0^{-+}\rangle \sim \|^3S_1,^{\bar{1}}\bar{P}_{\bar{1}};1,0,\rho\rangle$	8.1	1.63–1.73	8.6 ± 2.0	40–46	$2.55^{+0.21}_{-0.23}$	$X(2500)$
J_{17}^{1--}	$\|X_{17};1^{--}\rangle \sim \|^1S_0,^{\bar{3}}\bar{P}_{\bar{1}};1,1,\rho\rangle$	6.6	1.46–1.82	8.5 ± 2.0	40–61	$2.43^{+0.20}_{-0.24}$	$X(2400)$
J_{18}^{1--}	$\|X_{18};1^{--}\rangle \sim \|^3S_1,^{\bar{1}}\bar{P}_{\bar{1}};1,1,\rho\rangle$	7.4	1.67–1.88	8.5 ± 2.0	40–51	$2.44^{+0.20}_{-0.25}$	
J_{19}^{1-+}	$\|X_{19};1^{-+}\rangle \sim \|^1S_0,^{\bar{3}}\bar{P}_{\bar{1}};1,1,\rho\rangle$	8.0	1.68–1.77	8.5 ± 2.0	40–45	$2.49^{+0.21}_{-0.25}$	…
J_{20}^{1-+}	$\|X_{20};1^{-+}\rangle \sim \|^3S_1,^{\bar{1}}\bar{P}_{\bar{1}};1,1,\rho\rangle$	7.9	1.75–1.87	8.5 ± 2.0	40–46	$2.45^{+0.20}_{-0.25}$	…
J_{21}^{2--}	$\|X_{21};2^{--}\rangle \sim \|^1S_0,^{\bar{3}}\bar{P}_{\bar{2}};1,2,\rho\rangle$	4.2	1.39–1.89	8.5 ± 2.0	40–70	$2.36^{+0.20}_{-0.26}$	…
J_{22}^{2--}	$\|X_{22};2^{--}\rangle \sim \|^3S_1,^{\bar{1}}\bar{P}_{\bar{1}};1,2,\rho\rangle$	8.1	1.75–1.85	8.6 ± 2.0	40–45	$2.49^{+0.20}_{-0.24}$	…
J_{23}^{2-+}	$\|X_{23};2^{-+}\rangle \sim \|^1S_0,^{\bar{3}}\bar{P}_{\bar{2}};1,2,\rho\rangle$	6.4	1.49–1.86	8.5 ± 2.0	40–62	$2.38^{+0.20}_{-0.27}$	…
J_{24}^{2-+}	$\|X_{24};2^{-+}\rangle \sim \|^3S_1,^{\bar{1}}\bar{P}_{\bar{1}};1,2,\rho\rangle$	8.5	1.81–1.92	9.0 ± 2.0	40–45	$2.55^{+0.20}_{-0.24}$	…

$$M_{|X_1;0^{++}\rangle} = 2.11^{+0.19}_{-0.21}\ \text{GeV}. \tag{55}$$

Its central value corresponds to $s_0 = 6.5\ \text{GeV}^2$ and $M_B^2 = 1.71\ \text{GeV}^2$, and its uncertainty comes from the threshold value s_0, the Borel mass M_B, and various QCD parameters listed in Eqs. (48).

We repeat the same procedures to study the other 23 currents defined in Eqs. (12)–(14), Eqs. (16)–(23), and Eqs. (25)–(36). The obtained results are summarized in Table I, where we choose $s_0 = 6.5\ \text{GeV}^2$ for all the S-wave $ss\bar{s}\,\bar{s}$ tetraquark states, and $s_0 = 8.5$–$9.0\ \text{GeV}^2$ for some of the P-wave $ss\bar{s}\bar{s}$ tetraquark states. We shall use these results to draw conclusions in the next section. The minimum threshold value $s_0^{\min}$ is larger than $9.0\ \text{GeV}^2$ for the tetraquark currents $J^{\cdots}_{6,8,9,13,15}$, suggesting that their sum rule results may not be very well. Therefore, we shall not use them to draw conclusions, but note that this does not indicate the nonexistence of their corresponding tetraquark states $|X_{6,8,9,13,15}; J^{PC}\rangle$.

IV. SUMMARY AND DISCUSSIONS

In this paper we apply the QCD sum rule method to systematically study the S- and P-wave fully strange tetraquark states within the diquark-antidiquark picture. For the P-wave states, the orbital angular momentum can be between the diquark and antidiquark, or it can also be inside the diquark/antidiquark. We call the former λ-mode excitation and the latter ρ-mode excitation. There are altogether four S-wave $ss\bar{s}\bar{s}$ states, eight P-wave states of the λ-mode, and 12 P-wave states of the ρ-mode. We systematically construct their corresponding interpolating currents by explicitly adding the covariant derivative operator. We use these currents to perform QCD sum rule analyses, and the obtained results are summarized in Table I.

We compare our QCD sum rule results in Table II with those obtained in Refs. [38–42] using various quark models. Our QCD sum rule results are generally smaller than, but still more or less consistent with, the quark model calculation of Ref. [38]. Note that there can be significant mixing among the states with the same quantum number. This mixing effect has been systematically investigated in Ref. [38] through the nonrelativistic quark model, and it has also been partly investigated in Refs. [29–31,95] for the $J^{PC} = 0^{-+}/1^{-\pm}$ tetraquark states through the QCD sum rule method. However, a complete QCD sum rule study of the mixing effect is still not easy, so we do not systematically take it into account in the present study either.

TABLE II. Masses of the S- and P-wave fully strange tetraquark states, in units of MeV. Our QCD sum rule results are listed in the third column, and the quark model calculations taken from Refs. [38–42] are listed in the fourth through eighth columns.

Currents	Configuration	QCD sum rules	Ref. [38]	Ref. [39]	Ref. [40]	Ref. [41]	Ref. [42]
$J_1^{0^{++}}$	$\|X_1;0^{++}\rangle \sim \|^1S_0,^{\bar{1}}\bar{S}_{\bar{0}};J=0\rangle$	$2.11^{+0.19}_{-0.21}$	2365	⋯	1925	⋯	⋯
$J_2^{0^{++}}$	$\|X_2;0^{++}\rangle \sim \|^3S_1,^{\bar{3}}\bar{S}_{\bar{1}};J=0\rangle$	$1.99^{+0.19}_{-0.24}$	2293	1716	⋯	⋯	2203
$J_3^{1^{+-}}$	$\|X_3;1^{+-}\rangle \sim \|^3S_1,^{\bar{3}}\bar{S}_{\bar{1}};J=1\rangle$	$2.06^{+0.18}_{-0.20}$	2323	1960	⋯	⋯	2267
$J_4^{2^{++}}$	$\|X_4;2^{++}\rangle \sim \|^3S_1,^{\bar{3}}\bar{S}_{\bar{1}};J=2\rangle$	$2.09^{+0.19}_{-0.22}$	2378	2255	⋯	⋯	2357
$J_5^{0^{-+}}$	$\|X_5;0^{-+}\rangle \sim \|^3S_1,^{\bar{3}}\bar{S}_{\bar{1}};1,0,\lambda\rangle$	$2.31^{+0.21}_{-0.26}$	2576	2450	⋯	⋯	⋯
$J_6^{1^{--}}$	$\|X_6;1^{--}\rangle \sim \|^1S_0,^{\bar{1}}\bar{S}_{\bar{0}};0,1,\lambda\rangle$	⋯	2889	⋯	2290	⋯	⋯
$J_7^{1^{--}}$	$\|X_7;1^{--}\rangle \sim \|^3S_1,^{\bar{3}}\bar{S}_{\bar{1}};0,1,\lambda\rangle$	$2.34^{+0.23}_{-0.30}$	2636	2574	2188	2090/2333	⋯
$J_8^{1^{--}}$	$\|X_8;1^{--}\rangle \sim \|^3S_1,^{\bar{3}}\bar{S}_{\bar{1}};2,1,\lambda\rangle$	⋯	2584	2468	⋯	2000/2243	⋯
$J_9^{1^{-+}}$	$\|X_9;1^{-+}\rangle \sim \|^3S_1,^{\bar{3}}\bar{S}_{\bar{1}};1,1,\lambda\rangle$	⋯	2633	2581	⋯	⋯	⋯
$J_{10}^{2^{--}}$	$\|X_{10};2^{--}\rangle \sim \|^3S_1,^{\bar{3}}\bar{S}_{\bar{1}};2,2,\lambda\rangle$	$2.32^{+0.23}_{-0.30}$	2665	2622	⋯	⋯	⋯
$J_{11}^{2^{-+}}$	$\|X_{11};2^{-+}\rangle \sim \|^3S_1,^{\bar{3}}\bar{S}_{\bar{1}};1,2,\lambda\rangle$	$2.40^{+0.20}_{-0.25}$	2673	2619	⋯	⋯	⋯
$J_{12}^{3^{--}}$	$\|X_{12};3^{--}\rangle \sim \|^3S_1,^{\bar{3}}\bar{S}_{\bar{1}};2,3,\lambda\rangle$	$2.41^{+0.25}_{-0.30}$	2719	2660	⋯	⋯	⋯
$J_{13}^{0^{--}}$	$\|X_{13};0^{--}\rangle \sim \|^1S_0,^{\bar{3}}\bar{P}_{\bar{0}};1,0,\rho\rangle$	⋯	2635	⋯	⋯	⋯	⋯
$J_{14}^{0^{--}}$	$\|X_{14};0^{--}\rangle \sim \|^3S_1,^{\bar{1}}\bar{P}_{\bar{1}};1,0,\rho\rangle$	$2.50^{+0.21}_{-0.24}$	2694	2004	⋯	⋯	⋯
$J_{15}^{0^{-+}}$	$\|X_{15};0^{-+}\rangle \sim \|^1S_0,^{\bar{3}}\bar{P}_{\bar{0}};1,0,\rho\rangle$	⋯	2616	⋯	⋯	⋯	⋯
$J_{16}^{0^{-+}}$	$\|X_{16};0^{-+}\rangle \sim \|^3S_1,^{\bar{1}}\bar{P}_{\bar{1}};1,0,\rho\rangle$	$2.55^{+0.21}_{-0.23}$	2685	2004	⋯	⋯	⋯
$J_{17}^{1^{--}}$	$\|X_{17};1^{--}\rangle \sim \|^1S_0,^{\bar{3}}\bar{P}_{\bar{1}};1,1,\rho\rangle$	$2.43^{+0.20}_{-0.24}$	2585	⋯	⋯	⋯	⋯
$J_{18}^{1^{--}}$	$\|X_{18};1^{--}\rangle \sim \|^3S_1,^{\bar{1}}\bar{P}_{\bar{1}};1,1,\rho\rangle$	$2.44^{+0.20}_{-0.25}$	2694	2227	⋯	⋯	⋯
$J_{19}^{1^{-+}}$	$\|X_{19};1^{-+}\rangle \sim \|^1S_0,^{\bar{3}}\bar{P}_{\bar{1}};1,1,\rho\rangle$	$2.49^{+0.21}_{-0.25}$	2628	⋯	⋯	⋯	⋯
$J_{20}^{1^{-+}}$	$\|X_{20};1^{-+}\rangle \sim \|^3S_1,^{\bar{1}}\bar{P}_{\bar{1}};1,1,\rho\rangle$	$2.45^{+0.20}_{-0.25}$	2712	2227	⋯	⋯	⋯
$J_{21}^{2^{--}}$	$\|X_{21};2^{--}\rangle \sim \|^1S_0,^{\bar{3}}\bar{P}_{\bar{2}};1,2,\rho\rangle$	$2.36^{+0.20}_{-0.26}$	2620	⋯	⋯	⋯	⋯
$J_{22}^{2^{--}}$	$\|X_{22};2^{--}\rangle \sim \|^3S_1,^{\bar{1}}\bar{P}_{\bar{1}};1,2,\rho\rangle$	$2.49^{+0.20}_{-0.24}$	2725	2497	⋯	⋯	⋯
$J_{23}^{2^{-+}}$	$\|X_{23};2^{-+}\rangle \sim \|^1S_0,^{\bar{3}}\bar{P}_{\bar{2}};1,2,\rho\rangle$	$2.38^{+0.20}_{-0.27}$	2638	⋯	⋯	⋯	⋯
$J_{24}^{2^{-+}}$	$\|X_{24};2^{-+}\rangle \sim \|^3S_1,^{\bar{1}}\bar{P}_{\bar{1}};1,2,\rho\rangle$	$2.55^{+0.20}_{-0.24}$	2733	2497	⋯	⋯	⋯

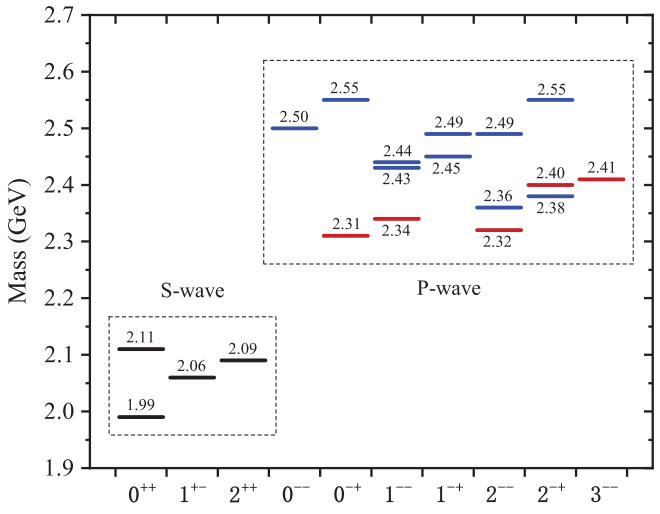

FIG. 6. Mass spectrum of the fully strange tetraquark states, including the S-wave states (black lines) as well as the P-wave states of the λ-mode (red lines) and the ρ-mode (blue lines).

Generally speaking, our results suggest that the S-wave $ss\bar{s}\bar{s}$ tetraquark states lie in the mass range of 1.99–2.11 GeV, and the P-wave states lie in the mass range of 2.31–2.55 GeV, as depicted in Fig. 6. The S-wave $ss\bar{s}\bar{s}$ tetraquark states decay into the $\eta'\eta'/\eta'\phi/\phi\phi$ channels through the S-wave, while the P-wave states decay into these channels through the P-wave, so the widths of the latter might be smaller than the former. As already discussed in Sec. I, there are some rich-strangeness signals at around 2.0 GeV, which are related to the fully strange tetraquark states with the quantum numbers $J^{PC} = 0^{++}$, 2^{++}, 1^{+-}, 0^{-+}, 1^{--}, and 1^{-+}. We separately discuss them as follows.

A. S-wave states of $J^{PC} = 0^{++}$ and 2^{++}

The S-wave $ss\bar{s}\bar{s}$ tetraquark states of $J^{PC} = 0^{++}$ and 2^{++} decay into the $\phi\phi$ channel through the S-wave. In 2016 the BESIII Collaboration performed a partial wave analysis of the $J/\psi \to \gamma\phi\phi$ decay, and observed one scalar resonance $f_0(2100)$ as well as three tensor resonances $f_2(2010)$, $f_2(2300)$, and $f_2(2340)$ in the $\phi\phi$ invariant mass spectrum [26]. Their masses and widths were measured to be

$$f_0(2100): M \approx 2101 \text{ MeV}, \quad \Gamma \approx 224 \text{ MeV}; \tag{56}$$

$$f_2(2010): M \approx 2011 \text{ MeV}, \quad \Gamma \approx 202 \text{ MeV}; \tag{57}$$

$$f_2(2300): M \approx 2297 \text{ MeV}, \quad \Gamma \approx 149 \text{ MeV}; \tag{58}$$

$$f_2(2340): M \approx 2339 \text{ MeV}, \quad \Gamma \approx 319 \text{ MeV}. \tag{59}$$

As depicted in Fig. 6, there are two S-wave $ss\bar{s}\bar{s}$ states of $J^{PC} = 0^{++}$, whose masses are calculated to be $1.99^{+0.19}_{-0.24}$ GeV and $2.11^{+0.19}_{-0.21}$ GeV. The latter one can be used to explain the scalar resonance $f_0(2100)$ as the S-wave $ss\bar{s}\bar{s}$ tetraquark state of $J^{PC} = 0^{++}$. There is one S-wave $ss\bar{s}\bar{s}$ state of $J^{PC} = 2^{++}$, whose mass is calculated to be $2.09^{+0.19}_{-0.22}$. It can be used to explain the tensor resonance $f_2(2010)$ as the S-wave $ss\bar{s}\bar{s}$ tetraquark state of $J^{PC} = 2^{++}$.

B. S-wave state of $J^{PC} = 1^{+-}$

The S-wave $ss\bar{s}\bar{s}$ tetraquark state of $J^{PC} = 1^{+-}$ decays into the $\phi\eta'$ channel through the S-wave. In 2018 the BESIII Collaboration observed the $X(2063)$ resonance in the $\phi\eta'$ invariant mass spectrum of the $J/\psi \to \phi\eta\eta'$ decay [27]. Its mass and width were measured to be

$$X(2063): M = 2062.8 \pm 13.1 \pm 7.2 \text{ MeV}, \quad \Gamma = 177 \pm 36 \pm 35 \text{ MeV}. \tag{60}$$

As depicted in Fig. 6, there is one S-wave $ss\bar{s}\bar{s}$ state of $J^{PC} = 1^{+-}$. Previously in Ref. [30], we used the current $J^{1^{+-}}_{3,\alpha}$ defined in Eq. (13) and applied the QCD sum rule method to calculate its mass to be $2.00^{+0.10}_{-0.09}$ GeV. In the present study we use the same current and calculate its mass to be $2.06^{+0.18}_{-0.20}$ GeV. These two results are well consistent with each other, both of which support the interpretation of the $X(2063)$ as the S-wave $ss\bar{s}\bar{s}$ tetraquark state of $J^{PC} = 1^{+-}$.

C. P-wave states of $J^{PC} = 0^{-+}$

The P-wave $ss\bar{s}\bar{s}$ tetraquark states of $J^{PC} = 0^{-+}$ decay into the $\phi\phi$ channel through the P-wave. In 2016 the BESIII Collaboration observed the $X(2500)$ resonance in the $\phi\phi$ invariant mass spectrum of the $J/\psi \to \gamma\phi\phi$ decay [26]. Besides, in 2010 the BESIII Collaboration observed two resonances $X(2120)$ and $X(2370)$ in the $\pi\pi\eta'$ invariant mass spectrum of the $J/\psi \to \gamma\pi\pi\eta'$ decay [24]. Later in 2019 they confirmed the $X(2370)$ in the $K\bar{K}\eta'$ invariant mass spectrum of the $J/\psi \to \gamma K\bar{K}\eta'$ decay, but they did not observe the $X(2120)$ in this process [25]. This suggests that the $X(2370)$ contains more strangeness components. The experimental parameters of the $X(2370)$ and $X(2500)$ were measured to be

$$X(2500): M = 2470^{+15\ +101}_{-19\ -23} \text{ MeV}, \quad \Gamma = 230^{+64\ +56}_{-35\ -33} \text{ MeV}; \tag{61}$$

$$X(2370): M = 2341.6 \pm 6.5 \pm 5.7 \text{ MeV}, \quad \Gamma = 117 \pm 10 \pm 8 \text{ MeV}. \tag{62}$$

Previously in Ref. [31] we applied the QCD sum rule method to study the $ss\bar{s}\bar{s}$ tetraquark states of $J^{PC} = 0^{-+}$ by investigating two independent currents without derivatives:

$$\eta_1 = (s_a^T C s_b)(\bar{s}_a \gamma_5 C \bar{s}_b^T) + (s_a^T C \gamma_5 s_b)(\bar{s}_a C \bar{s}_b^T),$$
$$\eta_2 = (s_a^T C \sigma_{\mu\nu} s_b)(\bar{s}_a \sigma^{\mu\nu} \gamma_5 C \bar{s}_b^T). \tag{63}$$

We took into account their mixing and further constructed two noncorrelated currents, based on which we calculated the masses to be $2.51^{+0.15}_{-0.12}$ GeV and $3.14^{+0.39}_{-0.26}$ GeV. The former one can be used to explain either the $X(2370)$ or $X(2500)$ as the P-wave $ss\bar{s}\bar{s}$ tetraquark state of $J^{PC} = 0^{-+}$.

In this study we use the $ss\bar{s}\bar{s}$ tetraquark currents with derivatives to perform QCD sum rule analyses. As shown in Fig. 2, there are three P-wave $ss\bar{s}\bar{s}$ tetraquark states of $J^{PC} = 0^{-+}$. We construct their corresponding currents, as defined in Eqs. (16), (27), and (28). Clearly, the use of the covariant derivative operator when constructing interpolating currents gives us more possibilities, based on which we can better describe the internal structure of multiquark states.

The two currents, $J_5^{0^{-+}}$ defined in Eq. (16) and $J_{16}^{0^{-+}}$ defined in Eq. (28), lead to reasonable QCD sum rule results. Their masses are calculated to be $2.31^{+0.21}_{-0.26}$ GeV and $2.55^{+0.21}_{-0.23}$ GeV, respectively. These results can be used to explain both the $X(2370)$ and $X(2500)$ as the P-wave $ss\bar{s}\bar{s}$ tetraquark states of $J^{PC} = 0^{-+}$.

D. P-wave states of $J^{PC} = 1^{--}$

The $\phi(2170)$ was first observed in 2006 by the *BABAR* Collaboration in the $\phi f_0(980)$ invariant mass spectrum [23,111–113], and later confirmed in the BESII/BESIII [114–124] and Belle [125] experiments. Besides, there might exist another structure in the $\phi f_0(980)$ invariant mass spectrum at around 2.4 GeV, whose evidences were observed in the *BABAR* [111], BESII/BESIII [114,115], and Belle [125,126] experiments.

Previously in Refs. [28,29] we applied the QCD sum rule method to study the $ss\bar{s}\bar{s}$ tetraquark states of $J^{PC} = 1^{--}$ by investigating two independent currents without derivatives:

$$\eta_{3\mu} = s_a^T C \gamma_5 s_b \bar{s}_a \gamma_\mu \gamma_5 C \bar{s}_b^T - s_a^T C \gamma_\mu \gamma_5 s_b \bar{s}_a \gamma_5 C \bar{s}_b^T,$$
$$\eta_{4\mu} = s_a^T C \gamma^\nu s_b \bar{s}_a \sigma_{\mu\nu} C \bar{s}_b^T - s_a^T C \sigma_{\mu\nu} s_b \bar{s}_a \gamma^\nu C \bar{s}_b^T. \tag{64}$$

We took into account their mixing and further constructed two noncorrelated currents, based on which we calculated the masses to be 2.34 ± 0.17 GeV and 2.41 ± 0.25 GeV. The former one was used to explain the $\phi(2170)$ as the S-wave $ss\bar{s}\bar{s}$ tetraquark state of $J^{PC} = 1^{--}$, and the latter one suggests that the $\phi(2170)$ has a partner state with the mass $\Delta M = 71^{+172}_{-48}$ MeV larger [29].

In a recent BESIII experiment the partner state of the $\phi(2170)$, labeled as $X(2400)$, was observed in the $e^+e^- \to \phi\pi^+\pi^-$ process with a statistical significance of 8.5σ [127]. The experimental parameters of the $\phi(2170)$ and $X(2400)$ were measured to be [1,127]

$$\phi(2170): M = 2160 \pm 80 \text{ MeV}, \quad \Gamma = 125 \pm 65 \text{ MeV}; \tag{65}$$

$$X(2400): M = 2298^{+60}_{-44} \pm 6 \text{ MeV}, \quad \Gamma = 219^{+117}_{-112} \pm 6 \text{ MeV}. \tag{66}$$

As shown in Fig. 2, there are as many as five P-wave $ss\bar{s}\bar{s}$ tetraquark states of $J^{PC} = 1^{--}$. In this study we construct their corresponding currents by explicitly adding the covariant derivative operator, as defined in Eqs. (17), (18), (19), (29), and (30). Three of them lead to reasonable QCD sum rule results, and the masses are calculated to be $2.34^{+0.23}_{-0.30}$ GeV, $2.43^{+0.20}_{-0.24}$ GeV, and $2.44^{+0.20}_{-0.25}$ GeV. Similar to our previous study of Ref. [29], these results can be used to explain both the $\phi(2170)$ and $X(2400)$ as the P-wave $ss\bar{s}\bar{s}$ tetraquark states of $J^{PC} = 1^{--}$.

E. P-wave states of $J^{PC} = 1^{-+}$

Very recently, the BESIII Collaboration studied the $J/\psi \to \gamma\eta\eta'$ decay process and observed the $\eta_1(1855)$ resonance with the exotic quantum number $I^G J^{PC} = 0^+1^{-+}$ in the $\eta\eta'$ invariant mass spectrum [84,85]. Its mass and width were measured to be

$$\eta_1(1855): M = 1855 \pm 9^{+6}_{-1} \text{ MeV}/c^2, \quad \Gamma = 188 \pm 18^{+3}_{-8} \text{ MeV}. \tag{67}$$

Previously in Refs. [95,96] we applied the QCD sum rule method to study the $qs\bar{q}\bar{s}$ ($q = u/d$) tetraquark states of $I^G J^{PC} = 0^+1^{-+}$ by investigating four independent currents without derivatives:

$$\eta_{5\mu} = u_a^T C \gamma_\mu s_b (\bar{u}_a C \bar{s}_b^T + \bar{u}_b C \bar{s}_a^T) + u_a^T C s_b (\bar{u}_a \gamma_\mu C \bar{s}_b^T + \bar{u}_b \gamma_\mu C \bar{s}_a^T) + \{u/\bar{u} \to d/\bar{d}\}, \tag{68}$$

$$\eta_{6\mu} = u_a^T C \sigma_{\mu\nu} \gamma_5 s_b (\bar{u}_a \gamma^\nu \gamma_5 C \bar{s}_b^T + \bar{u}_b \gamma^\nu \gamma_5 C \bar{s}_a^T) + u_a^T C \gamma^\nu \gamma_5 s_b (\bar{u}_a \sigma_{\mu\nu} \gamma_5 C \bar{s}_b^T + \bar{u}_b \sigma_{\mu\nu} \gamma_5 C \bar{s}_a^T) + \{u/\bar{u} \to d/\bar{d}\}, \tag{69}$$

$$\eta_{7\mu} = u_a^T C s_b (\bar{u}_a \gamma_\mu C \bar{s}_b^T - \bar{u}_b \gamma_\mu C \bar{s}_a^T) + u_a^T C \gamma_\mu s_b (\bar{u}_a C \bar{s}_b^T - \bar{u}_b C \bar{s}_a^T) + \{u/\bar{u} \to d/\bar{d}\}, \tag{70}$$

$$\eta_{8\mu} = u_a^T C\gamma^\nu\gamma_5 s_b(\bar{u}_a\sigma_{\mu\nu}\gamma_5 C\bar{s}_b^T - \bar{u}_b\sigma_{\mu\nu}\gamma_5 C\bar{s}_a^T) + u_a^T C\sigma_{\mu\nu}\gamma_5 s_b(\bar{u}_a\gamma^\nu\gamma_5 C\bar{s}_b^T - \bar{u}_b\gamma^\nu\gamma_5 C\bar{s}_a^T) + \{u/\bar{u} \to d/\bar{d}\}. \quad (71)$$

We took into account the mixing of $\eta_{5\mu}$ and $\eta_{7\mu}$, and calculated the mass to be around 1.8–2.1 GeV. This result can be used to explain the $\eta_1(1855)$ as the P-wave $qs\bar{q}\bar{s}$ tetraquark state of $I^GJ^{PC} = 0^+1^{-+}$. Based on this interpretation, one naturally expects the existence of the $ss\bar{s}\bar{s}$ tetraquark state of $I^GJ^{PC} = 0^+1^{-+}$.

As shown in Fig. 2, there are three P-wave $ss\bar{s}\bar{s}$ tetraquark states of $J^{PC} = 1^{-+}$. We construct their corresponding currents, two of which lead to reasonable QCD sum rule results. The masses extracted from the two currents, $J^{1^{-+}}_{19,\alpha\beta}$ defined in Eq. (31) and $J^{1^{-+}}_{20,\alpha\beta}$ defined in Eq. (32), are calculated to be $2.49^{+0.21}_{-0.25}$ GeV and $2.45^{+0.20}_{-0.25}$ GeV, respectively.

These states have the exotic quantum number $J^{PC} = 1^{-+}$, which cannot be accessed by conventional $\bar{q}q$ mesons, so they are of particular interest. We further study the mixing effect by investigating the off-diagonal correlation function

$$\langle 0|T[J^{1^{-+}}_{19,\mu\nu}(x)J^{1^{-+},\dagger}_{20,\rho\sigma}(0)]|0\rangle, \quad (72)$$

which is calculated to be zero. Therefore, the two currents $J^{1^{-+}}_{19,\alpha\beta}$ and $J^{1^{-+}}_{20,\alpha\beta}$ are noncorrelated, suggesting that there might exist two almost degenerate $ss\bar{s}\bar{s}$ tetraquark states with the exotic quantum number $J^{PC} = 1^{-+}$.

To end this paper, we propose to search for the S- and P-wave fully strange tetraquark states in the future Belle-II, BESIII, COMPASS, and GlueX experiments, etc. Besides the two-body decay channels $\eta\eta'/\phi\eta/\phi\eta'/\phi\phi/\phi f_0(980)$ already investigated in experiments, we propose to examine the two-body channels $\eta'\eta'/\eta f_0(980)/\eta' f_0(980)/f_0(980)f_0(980)$ and the relevant three-body channels.

ACKNOWLEDGMENTS

We thank Wei Chen, Er-Liang Cui, Wen-Biao Yan, and Shi-Lin Zhu for useful discussions. This project is supported by the National Natural Science Foundation of China under Grant No. 12075019, the Jiangsu Provincial Double-Innovation Program under Grant No. JSSCRC2021488, and the Fundamental Research Funds for the Central Universities.

APPENDIX: SPECTRAL DENSITIES

In this appendix we list the QCD sum rule equations extracted from the currents $J^{\cdots}_{2\cdots 24,\cdots}$ defined in Eqs. (12)–(14), Eqs. (16)–(23), and Eqs. (25)–(36).

$$\Pi_{22} = \int_{16m_s^2}^{s_0}\left[\frac{s^4}{15360\pi^6} - \frac{m_s^2 s^3}{256\pi^6} + \frac{\langle g_s^2GG\rangle}{3072\pi^6}s^2 + \left(-\frac{3\langle g_s^2GG\rangle m_s^2}{512\pi^6} - \frac{m_s\langle g_s\bar{s}\sigma Gs\rangle}{32\pi^4} + \frac{\langle\bar{s}s\rangle^2}{6\pi^2}\right)s + \frac{\langle g_s^2GG\rangle m_s\langle\bar{s}s\rangle}{64\pi^4} + \frac{7m_s^2\langle\bar{s}s\rangle^2}{6\pi^2} + \frac{\langle\bar{s}s\rangle\langle g_s\bar{s}\sigma Gs\rangle}{12\pi^2}\right]e^{-s/M^2}ds + \left(\frac{\langle g_s^2GG\rangle m_s\langle g_s\bar{s}\sigma Gs\rangle}{384\pi^4} - \frac{\langle g_s^2GG\rangle\langle\bar{s}s\rangle^2}{144\pi^2} + \frac{5m_s^2\langle\bar{s}s\rangle\langle g_s\bar{s}\sigma Gs\rangle}{8\pi^2} - \frac{4m_s\langle\bar{s}s\rangle^3}{3}\right) + \frac{1}{M_B^2}\left(-\frac{\langle g_s^2GG\rangle m_s^2\langle\bar{s}s\rangle^2}{576\pi^2} + \frac{\langle g_s^2GG\rangle\langle\bar{s}s\rangle\langle g_s\bar{s}\sigma Gs\rangle}{288\pi^2} - \frac{5m_s^2\langle g_s\bar{s}\sigma Gs\rangle^2}{48\pi^2} + \frac{7m_s\langle\bar{s}s\rangle^2\langle g_s\bar{s}\sigma Gs\rangle}{6}\right), \quad (A1)$$

$$\Pi_{33} = \int_{16m_s^2}^{s_0}\left[\frac{s^4}{12288\pi^6} - \frac{m_s^2 s^3}{2560\pi^6} + \left(\frac{\langle g_s^2GG\rangle}{18432\pi^6} - \frac{13m_s\langle\bar{s}s\rangle}{96\pi^4}\right)s^2 + \left(-\frac{\langle g_s^2GG\rangle m_s^2}{2304\pi^6} - \frac{155m_s\langle g_s\bar{s}\sigma Gs\rangle}{576\pi^4} + \frac{25\langle\bar{s}s\rangle^2}{36\pi^2}\right)s - \frac{13m_s^2\langle\bar{s}s\rangle^2}{8\pi^2} + \frac{31\langle\bar{s}s\rangle\langle g_s\bar{s}\sigma Gs\rangle}{48\pi^2}\right]e^{-s/M^2}ds + \left(\frac{11m_s^2\langle\bar{s}s\rangle\langle g_s\bar{s}\sigma Gs\rangle}{48\pi^2} - \frac{14m_s\langle\bar{s}s\rangle^3}{9} + \frac{\langle g_s\bar{s}\sigma Gs\rangle^2}{18\pi^2}\right) + \frac{1}{M_B^2}\left(-\frac{\langle g_s^2GG\rangle m_s^2\langle\bar{s}s\rangle^2}{576\pi^2} + \frac{13m_s^2\langle g_s\bar{s}\sigma Gs\rangle^2}{96\pi^2} + \frac{11m_s\langle\bar{s}s\rangle^2\langle g_s\bar{s}\sigma Gs\rangle}{36}\right), \quad (A2)$$

$$\Pi_{44} = \int_{16m_s^2}^{s_0}\left[\frac{s^4}{86016\pi^6} - \frac{m_s^2 s^3}{2880\pi^6} + \left(-\frac{11\langle g_s^2GG\rangle}{122880\pi^6} - \frac{3m_s\langle\bar{s}s\rangle}{320\pi^4}\right)s^2 + \left(\frac{5\langle g_s^2GG\rangle m_s^2}{9216\pi^6} - \frac{7m_s\langle g_s\bar{s}\sigma Gs\rangle}{288\pi^4} + \frac{\langle\bar{s}s\rangle^2}{18\pi^2}\right)s + \frac{11\langle g_s^2GG\rangle m_s\langle\bar{s}s\rangle}{6912\pi^4} + \frac{5m_s^2\langle\bar{s}s\rangle^2}{24\pi^2} + \frac{7\langle\bar{s}s\rangle\langle g_s\bar{s}\sigma Gs\rangle}{144\pi^2}\right]e^{-s/M^2}ds + \left(-\frac{\langle g_s^2GG\rangle\langle\bar{s}s\rangle^2}{432\pi^2} - \frac{4m_s\langle\bar{s}s\rangle^3}{9} + \frac{\langle g_s^2GG\rangle m_s\langle g_s\bar{s}\sigma Gs\rangle}{1152\pi^4} + \frac{m_s^2\langle\bar{s}s\rangle\langle g_s\bar{s}\sigma Gs\rangle}{4\pi^2}\right) + \frac{1}{M_B^2}\left(\frac{5\langle g_s^2GG\rangle m_s^2\langle\bar{s}s\rangle^2}{3457\pi^2} + \frac{5m_s^2\langle g_s\bar{s}\sigma Gs\rangle^2}{288\pi^2} + \frac{5m_s\langle\bar{s}s\rangle^2\langle g_s\bar{s}\sigma Gs\rangle}{54}\right), \tag{A3}$$

$$\Pi_{55} = \int_{16m_s^2}^{s_0}\left[\frac{7s^5}{307200\pi^6} - \frac{m_s^2 s^4}{2560\pi^6} - \frac{m_s\langle\bar{s}s\rangle}{32\pi^4}s^3 + \left(-\frac{\langle g_s^2GG\rangle m_s^2}{512\pi^6} + \frac{\langle\bar{s}s\rangle^2}{4\pi^2} - \frac{m_s\langle g_s\bar{s}\sigma Gs\rangle}{16\pi^4}\right)s^2 + \left(\frac{\langle g_s^2GG\rangle m_s\langle\bar{s}s\rangle}{96\pi^4} - \frac{19m_s^2\langle\bar{s}s\rangle^2}{8\pi^2} - \frac{\langle\bar{s}s\rangle\langle g_s\bar{s}\sigma Gs\rangle}{4\pi^2}\right)s + \frac{\langle g_s^2GG\rangle\langle\bar{s}s\rangle^2}{36\pi^2} - \frac{\langle g_s^2GG\rangle m_s\langle g_s\bar{s}\sigma Gs\rangle}{96\pi^4} - \frac{3m_s^2\langle\bar{s}s\rangle\langle g_s\bar{s}\sigma Gs\rangle}{2\pi^2} - \frac{\langle g_s\bar{s}\sigma Gs\rangle^2}{4\pi^2}\right]e^{-s/M^2}ds + \left(-\frac{\langle g_s^2GG\rangle m_s^2\langle\bar{s}s\rangle^2}{48\pi^2} + \frac{7\langle g_s^2GG\rangle\langle\bar{s}s\rangle\langle g_s\bar{s}\sigma Gs\rangle}{288\pi^2} + \frac{17m_s\langle\bar{s}s\rangle^2\langle g_s\bar{s}\sigma Gs\rangle}{6} - \frac{5m_s^2\langle g_s\bar{s}\sigma Gs\rangle^2}{16\pi^2}\right), \tag{A4}$$

$$\Pi_{66} = \int_{16m_s^2}^{s_0}\left[\frac{s^5}{358400\pi^6} - \frac{m_s^2 s^4}{7680\pi^6} + \left(-\frac{\langle g_s^2GG\rangle}{61440\pi^6} - \frac{m_s\langle\bar{s}s\rangle}{480\pi^4}\right)s^3 + \frac{\langle g_s^2GG\rangle m_s^2}{6144\pi^6}s^2 + \left(\frac{\langle g_s^2GG\rangle m_s\langle\bar{s}s\rangle}{1152\pi^4} - \frac{m_s^2\langle\bar{s}s\rangle^2}{36\pi^2} - \frac{\langle\bar{s}s\rangle\langle g_s\bar{s}\sigma Gs\rangle}{6\pi^2}\right)s + \frac{m_s^2\langle g_s\bar{s}\sigma Gs\rangle\langle\bar{s}s\rangle}{3\pi^2} - \frac{\langle g_s\bar{s}\sigma Gs\rangle^2}{8\pi^2}\right]e^{-s/M^2}ds + \left(\frac{\langle g_s^2GG\rangle m_s^2\langle\bar{s}s\rangle^2}{576\pi^2} + \frac{\langle g_s^2GG\rangle\langle\bar{s}s\rangle\langle g_s\bar{s}\sigma Gs\rangle}{288\pi^2} + \frac{4m_s\langle\bar{s}s\rangle^2\langle g_s\bar{s}\sigma Gs\rangle}{9} + \frac{m_s^2\langle g_s\bar{s}\sigma Gs\rangle^2}{6\pi^2}\right), \tag{A5}$$

$$\Pi_{77} = \int_{16m_s^2}^{s_0}\left[\frac{31s^5}{3225600\pi^6} - \frac{m_s^2 s^4}{1152\pi^6} + \left(\frac{\langle g_s^2GG\rangle}{9216\pi^6} + \frac{m_s\langle\bar{s}s\rangle}{160\pi^4}\right)s^3 + \left(-\frac{23\langle g_s^2GG\rangle m_s^2}{9216\pi^6} + \frac{m_s\langle g_s\bar{s}\sigma Gs\rangle}{192\pi^4}\right)s^2 + \left(\frac{\langle g_s^2GG\rangle m_s\langle\bar{s}s\rangle}{108\pi^4} + \frac{7m_s^2\langle\bar{s}s\rangle^2}{12\pi^2} - \frac{\langle\bar{s}s\rangle\langle g_s\bar{s}\sigma Gs\rangle}{6\pi^2}\right)s - \frac{\langle g_s\bar{s}\sigma Gs\rangle^2}{12\pi^2}\right]e^{-s/M^2}ds + \left(\frac{\langle g_s^2GG\rangle m_s^2\langle\bar{s}s\rangle^2}{432\pi^2} + \frac{\langle g_s^2GG\rangle\langle\bar{s}s\rangle\langle g_s\bar{s}\sigma Gs\rangle}{144\pi^2} + \frac{4m_s\langle\bar{s}s\rangle^2\langle g_s\bar{s}\sigma Gs\rangle}{3} - \frac{m_s^2\langle g_s\bar{s}\sigma Gs\rangle^2}{24\pi^2}\right), \tag{A6}$$

$$\Pi_{88} = \int_{16m_s^2}^{s_0}\left[\frac{19s^5}{5734400\pi^6} - \frac{23m_s^2 s^4}{92160\pi^6} + \left(\frac{7\langle g_s^2GG\rangle}{737280\pi^6} + \frac{23m_s\langle\bar{s}s\rangle}{7680\pi^4}\right)s^3 + \left(\frac{25\langle g_s^2GG\rangle m_s^2}{147456\pi^6} - \frac{\langle\bar{s}s\rangle^2}{72\pi^2} + \frac{37m_s\langle g_s\bar{s}\sigma Gs\rangle}{9216\pi^4}\right)s^2 + \left(-\frac{7\langle g_s^2GG\rangle m_s\langle\bar{s}s\rangle}{6912\pi^4} + \frac{11m_s^2\langle\bar{s}s\rangle^2}{192\pi^2} - \frac{25\langle\bar{s}s\rangle\langle g_s\bar{s}\sigma Gs\rangle}{216\pi^2}\right)s - \frac{m_s^2\langle\bar{s}s\rangle\langle g_s\bar{s}\sigma Gs\rangle}{64\pi^2} - \frac{17\langle g_s\bar{s}\sigma Gs\rangle^2}{384\pi^2}\right]e^{-s/M^2}ds + \left(-\frac{13\langle g_s^2GG\rangle m_s^2\langle\bar{s}s\rangle^2}{6912\pi^2} + \frac{13\langle g_s^2GG\rangle\langle\bar{s}s\rangle\langle g_s\bar{s}\sigma Gs\rangle}{6912\pi^2} + \frac{10m_s\langle\bar{s}s\rangle^2\langle g_s\bar{s}\sigma Gs\rangle}{27} - \frac{55m_s^2\langle g_s\bar{s}\sigma Gs\rangle^2}{1152\pi^2}\right), \tag{A7}$$

$$\Pi_{99} = \int_{16m_s^2}^{s_0} \left[\frac{s^5}{516096\pi^6} - \frac{7m_s^2 s^4}{46080\pi^6} + \left(\frac{23\langle g_s^2 GG\rangle}{737280\pi^6} + \frac{m_s\langle \bar{s}s\rangle}{384\pi^4} \right) s^3 + \left(-\frac{\langle g_s^2 GG\rangle m_s^2}{4096\pi^6} - \frac{\langle \bar{s}s\rangle^2}{72\pi^2} + \frac{53 m_s \langle g_s \bar{s}\sigma Gs\rangle}{9216\pi^4} \right) s^2 + \left(\frac{\langle g_s^2 GG\rangle m_s \langle \bar{s}s\rangle}{13824\pi^4} + \frac{5m_s^2\langle \bar{s}s\rangle^2}{144\pi^2} - \frac{\langle \bar{s}s\rangle\langle g_s\bar{s}\sigma Gs\rangle}{12\pi^2} \right) s + \frac{m_s^2\langle \bar{s}s\rangle\langle g_s\bar{s}\sigma Gs\rangle}{64\pi^2} - \frac{3\langle g_s\bar{s}\sigma Gs\rangle^2}{128\pi^2} \right] e^{-s/M^2} ds + \left(-\frac{5\langle g_s^2 GG\rangle m_s^2\langle \bar{s}s\rangle^2}{2304\pi^2} + \frac{\langle g_s^2 GG\rangle\langle \bar{s}s\rangle\langle g_s\bar{s}\sigma Gs\rangle}{1152\pi^2} + \frac{17 m_s\langle \bar{s}s\rangle^2\langle g_s\bar{s}\sigma Gs\rangle}{108} - \frac{7m_s^2\langle g_s\bar{s}\sigma Gs\rangle^2}{576\pi^2} \right), \tag{A8}$$

$$\Pi_{1010} = \int_{16m_s^2}^{s_0} \left[\frac{3s^5}{358400\pi^6} - \frac{m_s^2 s^4}{2304\pi^6} + \left(-\frac{143\langle g_s^2 GG\rangle}{1658880\pi^6} - \frac{m_s\langle \bar{s}s\rangle}{2880\pi^4} \right) s^3 + \left(\frac{7\langle g_s^2 GG\rangle m_s^2}{11520\pi^6} + \frac{\langle \bar{s}s\rangle^2}{36\pi^2} - \frac{151 m_s\langle g_s\bar{s}\sigma Gs\rangle}{11520\pi^4} \right) s^2 + \left(-\frac{\langle g_s^2 GG\rangle m_s\langle \bar{s}s\rangle}{3456\pi^4} - \frac{17m_s^2\langle \bar{s}s\rangle^2}{36\pi^2} - \frac{41\langle \bar{s}s\rangle\langle g_s\bar{s}\sigma Gs\rangle}{432\pi^2} \right) s + \frac{\langle g_s^2 GG\rangle\langle \bar{s}s\rangle^2}{1296\pi^2} - \frac{\langle g_s^2 GG\rangle m_s\langle g_s\bar{s}\sigma Gs\rangle}{1152\pi^2} - \frac{197m_s^2\langle \bar{s}s\rangle\langle g_s\bar{s}\sigma Gs\rangle}{432\pi^2} - \frac{37\langle g_s\bar{s}\sigma Gs\rangle^2}{864\pi^2} \right] e^{-s/M^2} ds + \left(-\frac{5\langle g_s^2 GG\rangle m_s^2\langle \bar{s}s\rangle^2}{1728\pi^2} + \frac{\langle g_s^2 GG\rangle\langle \bar{s}s\rangle\langle g_s\bar{s}\sigma Gs\rangle}{432\pi^2} + \frac{19 m_s\langle \bar{s}s\rangle^2\langle g_s\bar{s}\sigma Gs\rangle}{36} - \frac{m_s^2\langle g_s\bar{s}\sigma Gs\rangle^2}{8\pi^2} \right), \tag{A9}$$

$$\Pi_{1111} = \int_{16m_s^2}^{s_0} \left[\frac{13s^5}{1075200\pi^6} - \frac{23m_s^2 s^4}{53760\pi^6} + \left(-\frac{\langle g_s^2 GG\rangle}{138240\pi^6} - \frac{83 m_s\langle \bar{s}s\rangle}{4302\pi^4} \right) s^3 + \left(\frac{\langle g_s^2 GG\rangle m_s^2}{3072\pi^6} + \frac{8\langle \bar{s}s\rangle^2}{45\pi^2} - \frac{637 m_s\langle g_s\bar{s}\sigma Gs\rangle}{11520\pi^4} \right) s^2 + \left(-\frac{\langle g_s^2 GG\rangle m_s\langle \bar{s}s\rangle}{864\pi^4} - \frac{41m_s^2\langle \bar{s}s\rangle^2}{36\pi^2} + \frac{37\langle \bar{s}s\rangle\langle g_s\bar{s}\sigma Gs\rangle}{144\pi^2} \right) s + \frac{\langle g_s^2 GG\rangle\langle \bar{s}s\rangle^2}{432\pi^2} + \frac{\langle g_s^2 GG\rangle m_s\langle g_s\bar{s}\sigma Gs\rangle}{1152\pi^4} - \frac{133m_s^2\langle \bar{s}s\rangle\langle g_s\bar{s}\sigma Gs\rangle}{216\pi^2} + \frac{5\langle g_s\bar{s}\sigma Gs\rangle^2}{432\pi^2} \right] e^{-s/M^2} ds + \left(-\frac{\langle g_s^2 GG\rangle m_s^2\langle \bar{s}s\rangle^2}{432\pi^2} + \frac{\langle g_s^2 GG\rangle\langle \bar{s}s\rangle\langle g_s\bar{s}\sigma Gs\rangle}{288\pi^2} + \frac{55 m_s\langle \bar{s}s\rangle^2\langle g_s\bar{s}\sigma Gs\rangle}{36} - \frac{49m_s^2\langle g_s\bar{s}\sigma Gs\rangle^2}{144\pi^2} \right), \tag{A10}$$

$$\Pi_{1212} = \int_{16m_s^2}^{s_0} \left[\frac{s^5}{691200\pi^6} - \frac{5m_s^2 s^4}{64512\pi^6} + \left(-\frac{19\langle g_s^2 GG\rangle}{967680\pi^6} - \frac{m_s\langle \bar{s}s\rangle}{1890\pi^4} \right) s^3 + \left(\frac{\langle g_s^2 GG\rangle m_s^2}{2880\pi^6} - \frac{7m_s\langle g_s\bar{s}\sigma Gs\rangle}{7680\pi^4} \right) s^2 + \left(-\frac{\langle g_s^2 GG\rangle m_s\langle \bar{s}s\rangle}{1920\pi^4} + \frac{m_s^2\langle \bar{s}s\rangle^2}{30\pi^2} - \frac{18\langle \bar{s}s\rangle\langle g_s\bar{s}\sigma Gs\rangle}{18\pi^2} \right) s - \frac{m_s^2\langle \bar{s}s\rangle\langle g_s\bar{s}\sigma Gs\rangle}{288\pi^2} - \frac{55\langle g_s\bar{s}\sigma Gs\rangle^2}{1728\pi^2} \right] e^{-s/M^2} ds + \left(\frac{\langle g_s^2 GG\rangle\langle \bar{s}s\rangle\langle g_s\bar{s}\sigma Gs\rangle}{432\pi^2} + \frac{4m_s\langle \bar{s}s\rangle^2\langle g_s\bar{s}\sigma Gs\rangle}{9} - \frac{m_s^2\langle g_s\bar{s}\sigma Gs\rangle^2}{12\pi^2} \right), \tag{A11}$$

$$\Pi_{1313} = \int_{16m_s^2}^{s_0} \left[\frac{m_s^2 s^4}{3840\pi^6} - \frac{m_s^4 s^3}{96\pi^6} + \left(-\frac{\langle g_s^2 GG\rangle m_s^2}{1536\pi^6} + \frac{m_s\langle g_s\bar{s}\sigma Gs\rangle}{24\pi^4} \right) s^2 + \left(\frac{m_s^2\langle \bar{s}s\rangle^2}{3\pi^2} - \frac{\langle \bar{s}s\rangle\langle g_s\bar{s}\sigma Gs\rangle}{6\pi^2} \right) s - \frac{\langle g_s^2 GG\rangle m_s\langle g_s\bar{s}\sigma Gs\rangle}{192\pi^4} + \frac{m_s^2\langle \bar{s}s\rangle\langle g_s\bar{s}\sigma Gs\rangle}{3\pi^2} - \frac{\langle g_s\bar{s}\sigma Gs\rangle^2}{24\pi^2} \right] e^{-s/M^2} ds + \left(\frac{\langle g_s^2 GG\rangle m_s^2\langle \bar{s}s\rangle^2}{144\pi^2} + \frac{\langle g_s^2 GG\rangle\langle \bar{s}s\rangle\langle g_s\bar{s}\sigma Gs\rangle}{288\pi^2} + \frac{4m_s\langle \bar{s}s\rangle^2\langle g_s\bar{s}\sigma Gs\rangle}{3} - \frac{5m_s^2\langle g_s\bar{s}\sigma Gs\rangle^2}{24\pi^2} \right), \tag{A12}$$

$$\Pi_{1414} = \int_{16m_s^2}^{s_0}\left[\frac{s^5}{102400\pi^6} - \frac{m_s^2 s^4}{1280\pi^6} + \frac{\langle g_s^2 GG\rangle s^3}{12288\pi^6} + \left(-\frac{\langle g_s^2 GG\rangle m_s^2}{768\pi^6} + \frac{\langle \bar{s}s\rangle^2}{12\pi^2} - \frac{3m_s\langle g_s\bar{s}\sigma Gs\rangle}{64\pi^4}\right)s^2 + \left(-\frac{\langle g_s^2 GG\rangle m_s\langle \bar{s}s\rangle}{384\pi^4} - \frac{m_s^2\langle \bar{s}s\rangle^2}{24\pi^2} + \frac{7\langle \bar{s}s\rangle\langle g_s\bar{s}\sigma Gs\rangle}{48\pi^2}\right)s + \frac{\langle g_s^2 GG\rangle\langle \bar{s}s\rangle^2}{72\pi^2} - \frac{\langle g_s^2 GG\rangle m_s\langle g_s\bar{s}\sigma Gs\rangle}{96\pi^4} - \frac{3m_s^2\langle \bar{s}s\rangle\langle g_s\bar{s}\sigma Gs\rangle}{2\pi^2} - \frac{\langle g_s\bar{s}\sigma Gs\rangle^2}{48\pi^2}\right]e^{-s/M^2}ds + \left(\frac{\langle g_s^2 GG\rangle m_s^2\langle \bar{s}s\rangle^2}{192\pi^2} + \frac{\langle g_s^2 GG\rangle\langle \bar{s}s\rangle\langle g_s\bar{s}\sigma Gs\rangle}{144\pi^2} + \frac{29m_s\langle \bar{s}s\rangle^2\langle g_s\bar{s}\sigma Gs\rangle}{36} - \frac{7m_s^2\langle g_s\bar{s}\sigma Gs\rangle^2}{48\pi^2}\right), \tag{A13}$$

$$\Pi_{1515} = \int_{16m_s^2}^{s_0}\left[\frac{m_s^2 s^4}{3840\pi^6} - \frac{m_s^4 s^3}{96\pi^6} + \left(-\frac{\langle g_s^2 GG\rangle m_s^2}{1536\pi^6} + \frac{m_s\langle g_s\bar{s}\sigma Gs\rangle}{24\pi^4}\right)s^2 + \left(\frac{m_s^2\langle \bar{s}s\rangle^2}{3\pi^2} - \frac{\langle \bar{s}s\rangle\langle g_s\bar{s}\sigma Gs\rangle}{6\pi^2}\right)s - \frac{\langle g_s^2 GG\rangle m_s\langle g_s\bar{s}\sigma Gs\rangle}{192\pi^4} + \frac{m_s^2\langle \bar{s}s\rangle\langle g_s\bar{s}\sigma Gs\rangle}{3\pi^2} - \frac{\langle g_s\bar{s}\sigma Gs\rangle^2}{24\pi^2}\right]e^{-s/M^2}ds + \left(\frac{\langle g_s^2 GG\rangle m_s^2\langle \bar{s}s\rangle^2}{144\pi^2} + \frac{\langle g_s^2 GG\rangle\langle \bar{s}s\rangle\langle g_s\bar{s}\sigma Gs\rangle}{288\pi^2} + \frac{4m_s\langle \bar{s}s\rangle^2\langle g_s\bar{s}\sigma Gs\rangle}{3} - \frac{5m_s^2\langle g_s\bar{s}\sigma Gs\rangle^2}{24\pi^2}\right), \tag{A14}$$

$$\Pi_{1616} = \int_{16m_s^2}^{s_0}\left[\frac{s^5}{102400\pi^6} - \frac{m_s^2 s^4}{1280\pi^6} + \frac{\langle g_s^2 GG\rangle s^3}{12288\pi^6} + \left(-\frac{\langle g_s^2 GG\rangle m_s^2}{512\pi^6} + \frac{\langle \bar{s}s\rangle^2}{12\pi^2} - \frac{3m_s\langle g_s\bar{s}\sigma Gs\rangle}{64\pi^4}\right)s^2 + \left(\frac{\langle g_s^2 GG\rangle m_s\langle \bar{s}s\rangle}{384\pi^4} - \frac{m_s^2\langle \bar{s}s\rangle^2}{24\pi^2} + \frac{3\langle \bar{s}s\rangle\langle g_s\bar{s}\sigma Gs\rangle}{16\pi^2}\right)s + \frac{\langle g_s^2 GG\rangle\langle \bar{s}s\rangle^2}{72\pi^2} - \frac{\langle g_s^2 GG\rangle m_s\langle g_s\bar{s}\sigma Gs\rangle}{96\pi^4} - \frac{17m_s^2\langle \bar{s}s\rangle\langle g_s\bar{s}\sigma Gs\rangle}{12\pi^2} + \frac{\langle g_s\bar{s}\sigma Gs\rangle^2}{48\pi^2}\right]e^{-s/M^2}ds + \left(\frac{\langle g_s^2 GG\rangle m_s^2\langle \bar{s}s\rangle^2}{192\pi^2} + \frac{\langle g_s^2 GG\rangle\langle \bar{s}s\rangle\langle g_s\bar{s}\sigma Gs\rangle}{96\pi^2} + \frac{3m_s\langle \bar{s}s\rangle^2\langle g_s\bar{s}\sigma Gs\rangle}{4} - \frac{m_s^2\langle g_s\bar{s}\sigma Gs\rangle^2}{6\pi^2}\right), \tag{A15}$$

$$\Pi_{1717} = \int_{16m_s^2}^{s_0}\left[\frac{17s^5}{6451200\pi^6} - \frac{m_s^2 s^4}{5760\pi^6} + \left(-\frac{\langle g_s^2 GG\rangle}{61440\pi^6} - \frac{m_s\langle \bar{s}s\rangle}{720\pi^4}\right)s^3 + \left(\frac{\langle g_s^2 GG\rangle m_s^2}{12288\pi^6} + \frac{\langle \bar{s}s\rangle^2}{36\pi^2} - \frac{31m_s\langle g_s\bar{s}\sigma Gs\rangle}{4608\pi^4}\right)s^2 + \left(\frac{\langle g_s^2 GG\rangle m_s\langle \bar{s}s\rangle}{768\pi^4} - \frac{5m_s^2\langle \bar{s}s\rangle^2}{36\pi^2} + \frac{\langle \bar{s}s\rangle\langle g_s\bar{s}\sigma Gs\rangle}{27\pi^2}\right)s - \frac{5\langle g_s^2 GG\rangle\langle \bar{s}s\rangle^2}{3456\pi^2} - \frac{\langle g_s^2 GG\rangle m_s\langle g_s\bar{s}\sigma Gs\rangle}{1536\pi^4} - \frac{17m_s^2\langle \bar{s}s\rangle\langle g_s\bar{s}\sigma Gs\rangle}{144\pi^2} - \frac{\langle g_s\bar{s}\sigma Gs\rangle^2}{288\pi^2}\right]e^{-s/M^2}ds + \left(-\frac{\langle g_s^2 GG\rangle m_s^2\langle \bar{s}s\rangle^2}{3456\pi^2} + \frac{5\langle g_s^2 GG\rangle\langle \bar{s}s\rangle\langle g_s\bar{s}\sigma Gs\rangle}{6912\pi^2} + \frac{m_s\langle \bar{s}s\rangle^2\langle g_s\bar{s}\sigma Gs\rangle}{6} - \frac{m_s^2\langle g_s\bar{s}\sigma Gs\rangle^2}{16\pi^2}\right), \tag{A16}$$

$$\Pi_{1818} = \int_{16m_s^2}^{s_0}\left[\frac{13s^5}{12902400\pi^6} - \frac{m_s^2 s^4}{18432\pi^6} + \left(\frac{\langle g_s^2 GG\rangle}{368640\pi^6} - \frac{m_s\langle \bar{s}s\rangle}{960\pi^4}\right)s^3 + \left(-\frac{\langle g_s^2 GG\rangle m_s^2}{73728\pi^6} + \frac{\langle \bar{s}s\rangle^2}{72\pi^2} - \frac{11m_s\langle g_s\bar{s}\sigma Gs\rangle}{3072\pi^4}\right)s^2 + \left(-\frac{\langle g_s^2 GG\rangle m_s\langle \bar{s}s\rangle}{1152\pi^4} - \frac{m_s^2\langle \bar{s}s\rangle^2}{12\pi^2} + \frac{47\langle \bar{s}s\rangle\langle g_s\bar{s}\sigma Gs\rangle}{1728\pi^2}\right)s + \frac{5\langle g_s^2 GG\rangle\langle \bar{s}s\rangle^2}{3456\pi^2} - \frac{\langle g_s^2 GG\rangle m_s\langle g_s\bar{s}\sigma Gs\rangle}{1152\pi^4} - \frac{7m_s^2\langle \bar{s}s\rangle\langle g_s\bar{s}\sigma Gs\rangle}{72\pi^2} + \frac{5\langle g_s\bar{s}\sigma Gs\rangle^2}{1152\pi^2}\right]e^{-s/M^2}ds + \left(-\frac{\langle g_s^2 GG\rangle m_s^2\langle \bar{s}s\rangle^2}{1728\pi^2} + \frac{\langle g_s^2 GG\rangle\langle \bar{s}s\rangle\langle g_s\bar{s}\sigma Gs\rangle}{2304\pi^2} + \frac{61m_s\langle \bar{s}s\rangle^2\langle g_s\bar{s}\sigma Gs\rangle}{432} - \frac{29m_s^2\langle g_s\bar{s}\sigma Gs\rangle^2}{576\pi^2}\right), \tag{A17}$$

$$\Pi_{1919} = \int_{16m_s^2}^{s_0} \left[\frac{17s^5}{6451200\pi^6} - \frac{m_s^2 s^4}{5760\pi^6} + \left(-\frac{\langle g_s^2 GG\rangle}{61440\pi^6} - \frac{m_s\langle \bar{s}s\rangle}{720\pi^4} \right) s^3 + \left(\frac{13\langle g_s^2 GG\rangle m_s^2}{36864\pi^6} + \frac{\langle \bar{s}s\rangle^2}{36\pi^2} - \frac{41 m_s \langle g_s \bar{s}\sigma Gs\rangle}{4608\pi^4} \right) s^2 + \left(-\frac{11\langle g_s^2 GG\rangle m_s\langle \bar{s}s\rangle}{6912\pi^4} - \frac{5m_s^2\langle \bar{s}s\rangle^2}{36\pi^2} + \frac{13\langle \bar{s}s\rangle\langle g_s\bar{s}\sigma Gs\rangle}{216\pi^2} \right) s + \frac{5\langle g_s^2 GG\rangle\langle \bar{s}s\rangle^2}{3456\pi^2} - \frac{\langle g_s^2 GG\rangle m_s\langle g_s\bar{s}\sigma Gs\rangle}{1536\pi^4} - \frac{23 m_s^2\langle \bar{s}s\rangle\langle g_s\bar{s}\sigma Gs\rangle}{144\pi^2} + \frac{\langle g_s\bar{s}\sigma Gs\rangle^2}{72\pi^2} \right] e^{-s/M^2} ds + \left(-\frac{\langle g_s^2 GG\rangle m_s^2\langle \bar{s}s\rangle^2}{3456\pi^2} + \frac{5\langle g_s^2 GG\rangle\langle \bar{s}s\rangle\langle g_s\bar{s}\sigma Gs\rangle}{6912\pi^2} + \frac{m_s\langle \bar{s}s\rangle^2\langle g_s\bar{s}\sigma Gs\rangle}{6} - \frac{m_s^2\langle g_s\bar{s}\sigma Gs\rangle^2}{16\pi^2} \right), \tag{A18}$$

$$\Pi_{2020} = \int_{16m_s^2}^{s_0} \left[\frac{13s^5}{12902400\pi^6} - \frac{m_s^2 s^4}{18432\pi^6} + \left(\frac{\langle g_s^2 GG\rangle}{368640\pi^6} - \frac{m_s\langle \bar{s}s\rangle}{960\pi^4} \right) s^3 + \left(\frac{\langle g_s^2 GG\rangle m_s^2}{73728\pi^6} + \frac{\langle \bar{s}s\rangle^2}{72\pi^2} - \frac{35 m_s \langle g_s \bar{s}\sigma Gs\rangle}{9216\pi^4} \right) s^2 + \left(-\frac{\langle g_s^2 GG\rangle m_s\langle \bar{s}s\rangle}{864\pi^4} - \frac{m_s^2\langle \bar{s}s\rangle^2}{12\pi^2} + \frac{55\langle \bar{s}s\rangle\langle g_s\bar{s}\sigma Gs\rangle}{1728\pi^2} \right) s + \frac{7\langle g_s^2 GG\rangle\langle \bar{s}s\rangle^2}{3456\pi^2} - \frac{\langle g_s^2 GG\rangle m_s\langle g_s\bar{s}\sigma Gs\rangle}{1152\pi^4} - \frac{31 m_s^2\langle \bar{s}s\rangle\langle g_s\bar{s}\sigma Gs\rangle}{288\pi^2} + \frac{11\langle g_s\bar{s}\sigma Gs\rangle^2}{1152\pi^2} \right] e^{-s/M^2} ds + \left(-\frac{\langle g_s^2 GG\rangle m_s^2\langle \bar{s}s\rangle^2}{1728\pi^2} + \frac{7\langle g_s^2 GG\rangle\langle \bar{s}s\rangle\langle g_s\bar{s}\sigma Gs\rangle}{6912\pi^2} + \frac{61 m_s\langle \bar{s}s\rangle^2\langle g_s\bar{s}\sigma Gs\rangle}{432} - \frac{31 m_s^2\langle g_s\bar{s}\sigma Gs\rangle^2}{576\pi^2} \right), \tag{A19}$$

$$\Pi_{2121} = \int_{16m_s^2}^{s_0} \left[\frac{s^5}{307200\pi^6} - \frac{11 m_s^2 s^4}{64512\pi^6} + \left(-\frac{7\langle g_s^2 GG\rangle}{3317760\pi^6} - \frac{23 m_s\langle \bar{s}s\rangle}{8640\pi^4} \right) s^3 + \left(-\frac{7\langle g_s^2 GG\rangle m_s^2}{184320\pi^6} + \frac{\langle \bar{s}s\rangle^2}{30\pi^2} - \frac{7 m_s \langle g_s \bar{s}\sigma Gs\rangle}{960\pi^4} \right) s^2 + \left(-\frac{\langle g_s^2 GG\rangle m_s\langle \bar{s}s\rangle}{864\pi^4} - \frac{m_s^2\langle \bar{s}s\rangle^2}{24\pi^2} + \frac{7\langle \bar{s}s\rangle\langle g_s\bar{s}\sigma Gs\rangle}{288\pi^2} \right) s + \frac{\langle g_s^2 GG\rangle\langle \bar{s}s\rangle^2}{864\pi^2} - \frac{17\langle g_s^2 GG\rangle m_s\langle g_s\bar{s}\sigma Gs\rangle}{6912\pi^4} - \frac{25 m_s^2\langle \bar{s}s\rangle\langle g_s\bar{s}\sigma Gs\rangle}{216\pi^2} - \frac{17\langle g_s\bar{s}\sigma Gs\rangle^2}{864\pi^2} \right] e^{-s/M^2} ds + \left(\frac{\langle g_s^2 GG\rangle m_s^2\langle \bar{s}s\rangle^2}{3456\pi^2} - \frac{5\langle g_s^2 GG\rangle\langle \bar{s}s\rangle\langle g_s\bar{s}\sigma Gs\rangle}{3456\pi^2} + \frac{7 m_s\langle \bar{s}s\rangle^2\langle g_s\bar{s}\sigma Gs\rangle}{9} - \frac{43 m_s^2\langle g_s\bar{s}\sigma Gs\rangle^2}{288\pi^2} \right), \tag{A20}$$

$$\Pi_{2222} = \int_{16m_s^2}^{s_0} \left[\frac{3s^5}{1433600\pi^6} - \frac{11 m_s^2 s^4}{92160\pi^6} + \left(-\frac{\langle g_s^2 GG\rangle}{3317760\pi^6} - \frac{11 m_s\langle \bar{s}s\rangle}{5760\pi^4} \right) s^3 + \left(\frac{\langle g_s^2 GG\rangle m_s^2}{11520\pi^6} + \frac{\langle \bar{s}s\rangle^2}{36\pi^2} - \frac{209 m_s \langle g_s \bar{s}\sigma Gs\rangle}{23040\pi^4} \right) s^2 + \left(-\frac{7\langle g_s^2 GG\rangle m_s\langle \bar{s}s\rangle}{3456\pi^4} - \frac{7 m_s^2\langle \bar{s}s\rangle^2}{48\pi^2} + \frac{\langle \bar{s}s\rangle\langle g_s\bar{s}\sigma Gs\rangle}{16\pi^2} \right) s + \frac{\langle g_s^2 GG\rangle\langle \bar{s}s\rangle^2}{324\pi^2} - \frac{7\langle g_s^2 GG\rangle m_s\langle g_s\bar{s}\sigma Gs\rangle}{3456\pi^4} - \frac{7 m_s^2\langle \bar{s}s\rangle\langle g_s\bar{s}\sigma Gs\rangle}{27\pi^2} + \frac{19\langle g_s\bar{s}\sigma Gs\rangle^2}{1728\pi^2} \right] e^{-s/M^2} ds + \left(-\frac{\langle g_s^2 GG\rangle m_s^2\langle \bar{s}s\rangle^2}{3456\pi^2} + \frac{5\langle g_s^2 GG\rangle\langle \bar{s}s\rangle\langle g_s\bar{s}\sigma Gs\rangle}{3456\pi^2} + \frac{59 m_s\langle \bar{s}s\rangle^2\langle g_s\bar{s}\sigma Gs\rangle}{216} - \frac{m_s^2\langle g_s\bar{s}\sigma Gs\rangle^2}{12\pi^2} \right), \tag{A21}$$

$$\Pi_{2323} = \int_{16m_s^2}^{s_0} \left[\frac{s^5}{307200\pi^6} - \frac{11 m_s^2 s^4}{64512\pi^6} + \left(-\frac{7\langle g_s^2 GG\rangle}{3317760\pi^6} - \frac{23 m_s\langle \bar{s}s\rangle}{8640\pi^4} \right) s^3 + \left(-\frac{7\langle g_s^2 GG\rangle m_s^2}{184320\pi^6} + \frac{\langle \bar{s}s\rangle^2}{30\pi^2} - \frac{7 m_s \langle g_s \bar{s}\sigma Gs\rangle}{960\pi^4} \right) s^2 + \left(-\frac{\langle g_s^2 GG\rangle m_s\langle \bar{s}s\rangle}{864\pi^4} - \frac{m_s^2\langle \bar{s}s\rangle^2}{24\pi^2} + \frac{17\langle \bar{s}s\rangle\langle g_s\bar{s}\sigma Gs\rangle}{288\pi^2} \right) s + \frac{13\langle g_s^2 GG\rangle\langle \bar{s}s\rangle^2}{2592\pi^2} - \frac{17\langle g_s^2 GG\rangle m_s\langle g_s\bar{s}\sigma Gs\rangle}{6912\pi^4} - \frac{35 m_s^2\langle \bar{s}s\rangle\langle g_s\bar{s}\sigma Gs\rangle}{216\pi^2} + \frac{23\langle g_s\bar{s}\sigma Gs\rangle^2}{864\pi^2} \right] e^{-s/M^2} ds + \left(\frac{\langle g_s^2 GG\rangle m_s^2\langle \bar{s}s\rangle^2}{3456\pi^2} + \frac{5\langle g_s^2 GG\rangle\langle \bar{s}s\rangle\langle g_s\bar{s}\sigma Gs\rangle}{1152\pi^2} + \frac{7 m_s\langle \bar{s}s\rangle^2\langle g_s\bar{s}\sigma Gs\rangle}{9} - \frac{53 m_s^2\langle g_s\bar{s}\sigma Gs\rangle^2}{288\pi^2} \right), \tag{A22}$$

$$\Pi_{2424} = \int_{16m_s^2}^{s_0} \left[\frac{3s^5}{1433600\pi^6} - \frac{11m_s^2 s^4}{92160\pi^6} + \left(-\frac{\langle g_s^2 GG\rangle}{3317760\pi^6} - \frac{11m_s\langle \bar{s}s\rangle}{5760\pi^4} \right) s^3 + \left(\frac{\langle g_s^2 GG\rangle m_s^2}{11520\pi^6} + \frac{\langle \bar{s}s\rangle^2}{36\pi^2} - \frac{209 m_s \langle g_s \bar{s}\sigma Gs\rangle}{23040\pi^4} \right) s^2 + \left(-\frac{7\langle g_s^2 GG\rangle m_s \langle \bar{s}s\rangle}{3456\pi^4} - \frac{7m_s^2\langle \bar{s}s\rangle^2}{48\pi^2} + \frac{\langle \bar{s}s\rangle\langle g_s\bar{s}\sigma Gs\rangle}{16\pi^2} \right) s + \frac{\langle g_s^2 GG\rangle\langle \bar{s}s\rangle^2}{324\pi^2} - \frac{7\langle g_s^2 GG\rangle m_s\langle g_s\bar{s}\sigma Gs\rangle}{3456\pi^4} - \frac{7m_s^2\langle \bar{s}s\rangle\langle g_s\bar{s}\sigma Gs\rangle}{27\pi^2} + \frac{19\langle g_s\bar{s}\sigma Gs\rangle^2}{1728\pi^2} \right] e^{-s/M^2} ds + \left(-\frac{\langle g_s^2 GG\rangle m_s^2\langle \bar{s}s\rangle^2}{3456\pi^2} + \frac{5\langle g_s^2 GG\rangle\langle \bar{s}s\rangle\langle g_s\bar{s}\sigma Gs\rangle}{3456\pi^2} + \frac{59 m_s\langle \bar{s}s\rangle^2\langle g_s\bar{s}\sigma Gs\rangle}{216} - \frac{m_s^2\langle g_s\bar{s}\sigma Gs\rangle^2}{12\pi^2} \right). \quad \text{(A23)}$$

[1] M. Tanabashi *et al.* (Particle Data Group), Review of particle physics, Phys. Rev. D **98**, 030001 (2018).
[2] H. X. Chen, W. Chen, X. Liu, and S. L. Zhu, The hidden-charm pentaquark and tetraquark states, Phys. Rep. **639**, 1 (2016).
[3] Y. R. Liu, H. X. Chen, W. Chen, X. Liu, and S. L. Zhu, Pentaquark and tetraquark states, Prog. Part. Nucl. Phys. **107**, 237 (2019).
[4] H. X. Chen, W. Chen, X. Liu, Y. R. Liu, and S. L. Zhu, An updated review of the new hadron states, arXiv:2204.02649.
[5] R. F. Lebed, R. E. Mitchell, and E. S. Swanson, Heavy-quark QCD exotica, Prog. Part. Nucl. Phys. **93**, 143 (2017).
[6] A. Esposito, A. Pilloni, and A. D. Polosa, Multiquark resonances, Phys. Rep. **668**, 1 (2017).
[7] A. Hosaka, T. Iijima, K. Miyabayashi, Y. Sakai, and S. Yasui, Exotic hadrons with heavy flavors: X, Y, Z, and related states, Prog. Theor. Exp. Phys. **2016**, 062C01 (2016).
[8] F. K. Guo, C. Hanhart, U. G. Meissner, Q. Wang, Q. Zhao, and B. S. Zou, Hadronic molecules, Rev. Mod. Phys. **90**, 015004 (2018).
[9] A. Ali, J. S. Lange, and S. Stone, Exotics: Heavy pentaquarks and tetraquarks, Prog. Part. Nucl. Phys. **97**, 123 (2017).
[10] S. L. Olsen, T. Skwarnicki, and D. Zieminska, Nonstandard heavy mesons and baryons: Experimental evidence, Rev. Mod. Phys. **90**, 015003 (2018).
[11] M. Karliner, J. L. Rosner, and T. Skwarnicki, Multiquark States, Annu. Rev. Nucl. Part. Sci. **68**, 17 (2018).
[12] S. D. Bass and P. Moskal, η' and η mesons with connection to anomalous glue, Rev. Mod. Phys. **91**, 015003 (2019).
[13] N. Brambilla, S. Eidelman, C. Hanhart, A. Nefediev, C. P. Shen, C. E. Thomas, A. Vairo, and C. Z. Yuan, The XYZ states: Experimental and theoretical status and perspectives, Phys. Rep. **873**, 1 (2020).
[14] F. K. Guo, X. H. Liu, and S. Sakai, Threshold cusps and triangle singularities in hadronic reactions, Prog. Part. Nucl. Phys. **112**, 103757 (2020).
[15] B. Ketzer, B. Grube, and D. Ryabchikov, Light-meson spectroscopy with COMPASS, Prog. Part. Nucl. Phys. **113**, 103755 (2020).
[16] G. Yang, J. Ping, and J. Segovia, Tetra- and penta-quark structures in the constituent quark model, Symmetry **12**, 1869 (2020).
[17] C. D. Roberts, D. G. Richards, T. Horn, and L. Chang, Insights into the emergence of mass from studies of pion and kaon structure, Prog. Part. Nucl. Phys. **120**, 103883 (2021).
[18] S. s. Fang, B. Kubis, and A. Kupsc, What can we learn about light-meson interactions at electron–positron colliders?, Prog. Part. Nucl. Phys. **120**, 103884 (2021).
[19] S. Jin and X. Shen, Highlights of light meson spectroscopy at the BESIII experiment, Natl. Sci. Rev. **8**, nwab198 (2021).
[20] M. Albaladejo *et al.* (JPAC Collaboration), Novel approaches in Hadron Spectroscopy, 10.1016/j.ppnp.2022.103981.
[21] L. Meng, B. Wang, G. J. Wang, and S. L. Zhu, Chiral perturbation theory for heavy hadrons and chiral effective field theory for heavy hadronic molecules, arXiv:2204.08716.
[22] N. Brambilla, H. X. Chen, A. Esposito, J. Ferretti, A. Francis, F. K. Guo, C. Hanhart, A. Hosaka, R. L. Jaffe, M. Karliner *et al.*, Substructure of multiquark hadrons (Snowmass 2021 White Paper), arXiv:2203.16583.
[23] B. Aubert *et al.* (*BABAR* Collaboration), Structure at 2175 MeV in $e^+e^- \to \phi f_0(980)$ observed via initial-state radiation, Phys. Rev. D **74**, 091103 (2006).
[24] M. Ablikim *et al.* (BESIII Collaboration), Confirmation of the $X(1835)$ and Observation of the Resonances $X(2120)$ and $X(2370)$ in $J/\psi \to \gamma\pi^+\pi^-\eta'$, Phys. Rev. Lett. **106**, 072002 (2011).
[25] M. Ablikim *et al.* (BESIII Collaboration), Observation of $X(2370)$ and search for $X(2120)$ in $J/\psi \to \gamma K\bar{K}\eta'$, Eur. Phys. J. C **80**, 746 (2020).
[26] M. Ablikim *et al.* (BESIII Collaboration), Observation of pseudoscalar and tensor resonances in $J/\psi \to \gamma\phi\phi$, Phys. Rev. D **93**, 112011 (2016).
[27] M. Ablikim *et al.* (BESIII Collaboration), Observation and study of the decay $J/\psi \to \phi\eta\eta'$, Phys. Rev. D **99**, 112008 (2019).
[28] H. X. Chen, X. Liu, A. Hosaka, and S. L. Zhu, The $Y(2175)$ state in the QCD sum rule, Phys. Rev. D **78**, 034012 (2008).

[29] H. X. Chen, C. P. Shen, and S. L. Zhu, Possible partner state of the $Y(2175)$, Phys. Rev. D **98**, 014011 (2018).

[30] E. L. Cui, H. M. Yang, H. X. Chen, W. Chen, and C. P. Shen, QCD sum rule studies of $ss\bar{s}\bar{s}$ tetraquark states with $J^{PC} = 1^{+-}$, Eur. Phys. J. C **79**, 232 (2019).

[31] R. R. Dong, N. Su, H. X. Chen, E. L. Cui, and Z. Y. Zhou, QCD sum rule studies on the $ss\bar{s}\bar{s}$ tetraquark states of $J^{PC} = 0^{-+}$, Eur. Phys. J. C **80**, 749 (2020).

[32] R. R. Dong, N. Su, and H. X. Chen, Fully-strange tetraquark states with the exotic quantum number $J^{PC} = 4^{+-}$, arXiv:2206.09517.

[33] Z. G. Wang, Analysis of $Y(2175)$ as a tetraquark state with QCD sum rules, Nucl. Phys. **A791**, 106 (2007).

[34] Z. G. Wang, Light tetraquark state candidates, Adv. High Energy Phys. **2020**, 6438730 (2020).

[35] S. S. Agaev, K. Azizi, and H. Sundu, Nature of the vector resonance $Y(2175)$, Phys. Rev. D **101**, 074012 (2020).

[36] K. Azizi, S. S. Agaev, and H. Sundu, Light axial-vector and vector resonances $X(2100)$ and $X(2239)$, Nucl. Phys. **B948**, 114789 (2019).

[37] A. V. Pimikov, Nonlocal gluon condensates in QCD sum rules, arXiv:2205.12948.

[38] F. X. Liu, M. S. Liu, X. H. Zhong, and Q. Zhao, Fully strange tetraquark $ss\bar{s}\bar{s}$ spectrum and possible experimental evidence, Phys. Rev. D **103**, 016016 (2021).

[39] Q. F. Lü, K. L. Wang, and Y. B. Dong, The $ss\bar{s}\bar{s}$ tetraquark states and the structure of $X(2239)$ observed by the BESIII collaboration, Chin. Phys. C **44**, 024101 (2020).

[40] C. Deng, J. Ping, F. Wang, and T. Goldman, Tetraquark state and multibody interaction, Phys. Rev. D **82**, 074001 (2010).

[41] N. V. Drenska, R. Faccini, and A. D. Polosa, Higher tetraquark particles, Phys. Lett. B **669**, 160 (2008).

[42] D. Ebert, R. N. Faustov, and V. O. Galkin, Masses of light tetraquarks and scalar mesons in the relativistic quark model, Eur. Phys. J. C **60**, 273 (2009).

[43] M. Napsuciale, E. Oset, K. Sasaki, and C. A. Vaquera-Araujo, Electron-positron annihilation into $\phi f_0(980)$ and clues for a new 1^{--} resonance, Phys. Rev. D **76**, 074012 (2007).

[44] S. Gomez-Avila, M. Napsuciale, and E. Oset, ϕK^+K^- production in electron-positron annihilation, Phys. Rev. D **79**, 034018 (2009).

[45] A. Martinez Torres, K. P. Khemchandani, L. S. Geng, M. Napsuciale, and E. Oset, $X(2175)$ as a resonant state of the $\phi K\bar{K}$ system, Phys. Rev. D **78**, 074031 (2008).

[46] L. Alvarez-Ruso, J. A. Oller, and J. M. Alarcon, $\phi(1020)f_0(980)S$-wave scattering and the $Y(2175)$ resonance, Phys. Rev. D **80**, 054011 (2009).

[47] S. Coito, G. Rupp, and E. van Beveren, Multichannel calculation of excited vector ϕ resonances and the $\phi(2170)$, Phys. Rev. D **80**, 094011 (2009).

[48] J. J. Xie, A. Martinez Torres, and E. Oset, Faddeev fixed-center approximation to the $N\bar{K}K$ system and the signature of a $N^*(1920)(1/2^+)$ state, Phys. Rev. C **83**, 065207 (2011).

[49] G. J. Ding and M. L. Yan, $Y(2175)$: Distinguish hybrid state from higher quarkonium, Phys. Lett. B **657**, 49 (2007).

[50] C. Q. Pang, Excited states of ϕ meson, Phys. Rev. D **99**, 074015 (2019).

[51] C. Q. Pang, Y. R. Wang, J. F. Hu, T. J. Zhang, and X. Liu, Study of the ω meson family and newly observed ω-like state $X(2240)$, Phys. Rev. D **101**, 074022 (2020).

[52] L. M. Wang, S. Q. Luo, and X. Liu, Light unflavored vector meson spectroscopy around the mass range of 2.4–3 GeV and possible experimental evidence, Phys. Rev. D **105**, 034011 (2022).

[53] M. Abud, F. Buccella, and F. Tramontano, Hints for the existence of hexaquark states in the baryon-antibaryon sector, Phys. Rev. D **81**, 074018 (2010).

[54] L. Zhao, N. Li, S. L. Zhu, and B. S. Zou, Meson-exchange model for the $\Lambda\bar{\Lambda}$ interaction, Phys. Rev. D **87**, 054034 (2013).

[55] J. T. Zhu, Y. Liu, D. Y. Chen, L. Jiang, and J. He, $X(2239)$ and $\eta(2225)$ as hidden-strange molecular states from $\Lambda\bar{\Lambda}$ interaction, Chin. Phys. C **44**, 123103 (2020).

[56] G. J. Ding and M. L. Yan, A candidate for 1^{--} strangeonium hybrid, Phys. Lett. B **650**, 390 (2007).

[57] J. S. Yu, Z. F. Sun, X. Liu, and Q. Zhao, Categorizing resonances $X(1835)$, $X(2120)$ and $X(2370)$ in the pseudoscalar meson family, Phys. Rev. D **83**, 114007 (2011).

[58] W. I. Eshraim, S. Janowski, F. Giacosa, and D. H. Rischke, Decay of the pseudoscalar glueball into scalar and pseudoscalar mesons, Phys. Rev. D **87**, 054036 (2013).

[59] L. C. Gui, J. M. Dong, Y. Chen, and Y. B. Yang, Study of the pseudoscalar glueball in J/ψ radiative decays, Phys. Rev. D **100**, 054511 (2019).

[60] J. F. Liu, G.-J. Ding, and M.-L. Yan (BES Collaboration), $X(1835)$ and the new resonances $X(2120)$ and $X(2370)$ observed by the BES collaboration, Phys. Rev. D **82**, 074026 (2010).

[61] C. Deng, J. Ping, Y. Yang, and F. Wang, $X(1835)$, $X(2120)$ and $X(2370)$ in flux tube models, Phys. Rev. D **86**, 014008 (2012).

[62] B. D. Wan, S. Q. Zhang, and C. F. Qiao, Light baryonium spectrum, Phys. Rev. D **105**, 014016 (2022).

[63] T. T. Pan, Q. F. Lü, E. Wang, and D. M. Li, Strong decays of the $X(2500)$ newly observed by the BESIII Collaboration, Phys. Rev. D **94**, 054030 (2016).

[64] L. M. Wang, S. Q. Luo, Z. F. Sun, and X. Liu, Constructing new pseudoscalar meson nonets with the observed $X(2100)$, $X(2500)$, and $\eta(2225)$, Phys. Rev. D **96**, 034013 (2017).

[65] S. C. Xue, G. Y. Wang, G. N. Li, E. Wang, and D. M. Li, The possible members of the 5^1S_0 meson nonet, Eur. Phys. J. C **78**, 479 (2018).

[66] L. M. Wang, Q. S. Zhou, C. Q. Pang, and X. Liu, Potential higher radial excitations in the light pseudoscalar meson family, Phys. Rev. D **102**, 114034 (2020).

[67] Q. Li, L. C. Gui, M. S. Liu, Q. F. Lü, and X. H. Zhong, Mass spectrum and strong decays of strangeonium in a constituent quark model, Chin. Phys. C **45**, 023116 (2021).

[68] L. M. Wang, J. Z. Wang, S. Q. Luo, J. He, and X. Liu, Studying $X(2100)$ hadronic decays and predicting its pion and kaon induced productions, Phys. Rev. D **101**, 034021 (2020).

[69] C. J. Morningstar and M. J. Peardon, Glueball spectrum from an anisotropic lattice study, Phys. Rev. D **60**, 034509 (1999).

[70] Y. Chen, A. Alexandru, S. J. Dong, T. Draper, I. Horvath, F. X. Lee, K. F. Liu, N. Mathur, C. Morningstar, M. Peardon *et al.*, Glueball spectrum and matrix elements on anisotropic lattices, Phys. Rev. D **73**, 014516 (2006).

[71] C. M. Richards, A. C. Irving, E. B. Gregory, and C. McNeile (UKQCD Collaboration), Glueball mass measurements from improved staggered fermion simulations, Phys. Rev. D **82**, 034501 (2010).

[72] J. J. Dudek, The lightest hybrid meson supermultiplet in QCD, Phys. Rev. D **84**, 074023 (2011).

[73] E. Gregory, A. Irving, B. Lucini, C. McNeile, A. Rago, C. Richards, and E. Rinaldi, Towards the glueball spectrum from unquenched lattice QCD, J. High Energy Phys. 10 (2012) 170.

[74] W. I. Eshraim and S. Schramm, Decay modes of the excited pseudoscalar glueball, Phys. Rev. D **95**, 014028 (2017).

[75] W. I. Eshraim, Decay of the pseudoscalar glueball and its first excited state into scalar and pseudoscalar mesons and their first excited states, Phys. Rev. D **100**, 096007 (2019).

[76] D. Y. Chen, X. Liu, and T. Matsuki, Two charged strangeonium-like structures observable in the $Y(2175) \to \phi(1020)\pi^+\pi^-$ process, Eur. Phys. J. C **72**, 2008 (2012).

[77] X. Wang, Z. F. Sun, D. Y. Chen, X. Liu, and T. Matsuki, Nonstrange partner of strangeonium-like state $Y(2175)$, Phys. Rev. D **85**, 074024 (2012).

[78] W. Liang, C. W. Xiao, and E. Oset, Study of $\eta K\bar{K}$ and $\eta' K\bar{K}$ with the fixed center approximation to Faddeev equations, Phys. Rev. D **88**, 114024 (2013).

[79] A. A. Kozhevnikov, Dynamical analysis of the X resonance contributions to the decay $J/\psi \to \gamma X \to \gamma\phi\phi$, Phys. Rev. D **99**, 014019 (2019).

[80] P. Lebiedowicz, O. Nachtmann, and A. Szczurek, Central exclusive diffractive production of $K^+K^-K^+K^-$ via the intermediate $\phi\phi$ state in proton-proton collisions, Phys. Rev. D **99**, 094034 (2019).

[81] A. A. Kozhevnikov, The decay $J/\psi \to \gamma\phi\phi$: Spin dependence of amplitude and angular distributions of photons with linear polarizations, Eur. Phys. J. A **55**, 155 (2019).

[82] S. F. Chen and B. C. Liu, The $\gamma p \to \phi\eta' p$ reaction in an effective Lagrangian model, Phys. Rev. C **102**, 025202 (2020).

[83] X. Sun, L. Y. Dai, S. Q. Kuang, W. Qin, and A. P. Szczepaniak, Nature of $X(2370)$, Phys. Rev. D **105**, 034010 (2022).

[84] M. Ablikim *et al.* (BESIII Collaboration), Observation of an isoscalar resonance with exotic $J^{PC} = 1^{-+}$ quantum numbers in $J/\psi \to \gamma\eta\eta'$, arXiv:2202.00621.

[85] M. Ablikim *et al.* (BESIII Collaboration), Partial wave analysis of $J/\psi \to \gamma\eta\eta'$, Phys. Rev. D **105**, 072002 (2022).

[86] H. X. Chen, Z. X. Cai, P. Z. Huang, and S. L. Zhu, Decay properties of the 1^{-+} hybrid state, Phys. Rev. D **83**, 014006 (2011).

[87] P. Z. Huang, H. X. Chen, and S. L. Zhu, Strong decay patterns of the 1^{-+} exotic hybrid mesons, Phys. Rev. D **83**, 014021 (2011).

[88] H. X. Chen, N. Su, and S. L. Zhu, QCD axial anomaly enhances the $\eta\eta'$ decay of the hybrid candidate $\eta_1(1855)$, Chin. Phys. Lett. **39**, 051201 (2022).

[89] L. Qiu and Q. Zhao, Towards the establishment of the light $J^{P(C)} = 1^{-(+)}$ hybrid nonet, Chin. Phys. C **46**, 051001 (2022).

[90] V. Shastry, C. S. Fischer, and F. Giacosa, The phenomenology of the exotic hybrid nonet with $\pi_1(1600)$ and $\eta_1(1855)$, arXiv:2203.04327.

[91] X. K. Dong, Y. H. Lin, and B. S. Zou, Interpretation of the $\eta_1(1855)$ as a $K\bar{K}_1(1400) + \text{c.c.}$ molecule, Sci. China Phys. Mech. Astron. **65**, 261011 (2022).

[92] F. Yang and Y. Huang, Analysis of the $\eta_1(1855)$ as a $K\bar{K}_1(1400)$ molecular state, arXiv:2203.06934.

[93] B. D. Wan, S. Q. Zhang, and C. F. Qiao, A possible structure of newly found exotic state $\eta_1(1855)$, arXiv:2203.14014.

[94] X. Zhang and J. J. Xie, Prediction of possible exotic states in the $\eta\bar{K}K^*$ system, Chin. Phys. C **44**, 054104 (2020).

[95] H. X. Chen, A. Hosaka, and S. L. Zhu, $I^G J^{PC} = 0^+1^{-+}$ tetraquark state, Phys. Rev. D **78**, 117502 (2008).

[96] H. X. Chen, A. Hosaka, and S. L. Zhu, $I^G J^{PC} = 1^-1^{-+}$ tetraquark states, Phys. Rev. D **78**, 054017 (2008).

[97] M. A. Shifman, A. I. Vainshtein, and V. I. Zakharov, QCD and resonance physics. theoretical foundations, Nucl. Phys. **B147**, 385 (1979).

[98] L. J. Reinders, H. Rubinstein, and S. Yazaki, Hadron properties from QCD sum rules, Phys. Rep. **127**, 1 (1985).

[99] M. A. Shifman, A. I. Vainshtein, and V. I. Zakharov, QCD and resonance physics. applications, Nucl. Phys. **B147**, 448 (1979).

[100] M. A. Shifman, A. I. Vainshtein, and V. I. Zakharov, QCD and resonance physics. the $\rho - \omega$ mixing, Nucl. Phys. **B147**, 519 (1979).

[101] V. A. Novikov, M. A. Shifman, A. I. Vainshtein, and V. I. Zakharov, Calculations in external fields in quantum chromodynamics. technical review, Fortschr. Phys. **32**, 585 (1984).

[102] A. G. Grozin, Methods of calculation of higher power corrections in QCD, Int. J. Mod. Phys. A **10**, 3497 (1995).

[103] A. Grozin, *Lectures on QED and QCD: Practical Calculation and Renormalization of One- and Multi-Loop Feynman Diagrams* (World Scientific, Singapore, 2007).

[104] K. C. Yang, W. Y. P. Hwang, E. M. Henley, and L. S. Kisslinger, QCD sum rules and neutron proton mass difference, Phys. Rev. D **47**, 3001 (1993).

[105] S. Narison, QCD as a theory of hadrons (from partons to confinement), Cambridge Monogr. Part. Phys., Nucl. Phys., Cosmol. **17**, 1 (2002).

[106] V. Gimenez, V. Lubicz, F. Mescia, V. Porretti, and J. Reyes, Operator product expansion and quark condensate from lattice QCD in coordinate space, Eur. Phys. J. C **41**, 535 (2005).

[107] M. Jamin, Flavor-symmetry breaking of the quark condensate and chiral corrections to the Gell-Mann-Oakes-Renner relation, Phys. Lett. B **538**, 71 (2002).

[108] B. L. Ioffe and K. N. Zyablyuk, Gluon condensate in charmonium sum rules with three-loop corrections, Eur. Phys. J. C **27**, 229 (2003).

[109] A. A. Ovchinnikov and A. A. Pivovarov, QCD sum rule calculation of the quark gluon condensate, Sov. J. Nucl. Phys. **48**, 721 (1988).

[110] J. R. Ellis, E. Gardi, M. Karliner, and M. A. Samuel, Renormalization scheme dependence of Pade summation in QCD, Phys. Rev. D **54**, 6986 (1996).

[111] B. Aubert *et al.* (*BABAR* Collaboration), $e^+e^- \to K^+K^-\pi^+\pi^-$, $K^+K^-\pi^0\pi^0$ and $K^+K^-K^+K^-$ cross-sections measured with initial-state radiation, Phys. Rev. D **76**, 012008 (2007).

[112] B. Aubert *et al.* (*BABAR* Collaboration), Measurements of $e^+e^- \to K^+K^-\eta$, $K^+K^-\pi^0$ and $K^0_sK^\pm\pi^\mp$ cross-sections using initial state radiation events, Phys. Rev. D **77**, 092002 (2008).

[113] J. P. Lees *et al.* (*BABAR* Collaboration), Cross sections for the reactions $e^+e^- \to K^+K^-\pi^+\pi^-$, $K^+K^-\pi^0\pi^0$, and $K^+K^-K^+K^-$ measured using initial-state radiation events, Phys. Rev. D **86**, 012008 (2012).

[114] M. Ablikim *et al.* (BES Collaboration), Observation of $Y(2175)$ in $J\psi \to \eta\phi f_0(980)$, Phys. Rev. Lett. **100**, 102003 (2008).

[115] M. Ablikim *et al.* (BESIII Collaboration), Study of $J/\psi \to \eta\phi\pi^+\pi^-$ at BESIII, Phys. Rev. D **91**, 052017 (2015).

[116] M. Ablikim *et al.* (BESIII Collaboration), Observation of $e^+e^- \to \eta Y(2175)$ at center-of-mass energies above 3.7 GeV, Phys. Rev. D **99**, 012014 (2019).

[117] M. Ablikim *et al.* (BESIII Collaboration), Measurement of $e^+e^- \to K^+K^-$ cross section at $\sqrt{s} = 2.00$–3.08 GeV, Phys. Rev. D **99**, 032001 (2019).

[118] M. Ablikim *et al.* (BESIII Collaboration), Cross section measurements of $e^+e^- \to K^+K^-K^+K^-$ and ϕK^+K^- at center-of-mass energies from 2.10 to 3.08 GeV, Phys. Rev. D **100**, 032009 (2019).

[119] M. Ablikim *et al.* (BESIII Collaboration), Observation of a Resonant Structure in $e^+e^- \to K^+K^-\pi^0\pi^0$, Phys. Rev. Lett. **124**, 112001 (2020).

[120] M. Ablikim *et al.* (BESIII Collaboration), Observation of a structure in $e^+e^- \to \phi\eta'$ at $\sqrt{s}$ from 2.05 to 3.08 GeV, Phys. Rev. D **102**, 012008 (2020).

[121] M. Ablikim *et al.* (BESIII Collaboration), Observation of a resonant structure in $e^+e^- \to \omega\eta$ and another in $e^+e^- \to \omega\pi^0$ at center-of-mass energies between 2.00 and 3.08 GeV, Phys. Lett. B **813**, 136059 (2021).

[122] M. Ablikim *et al.* (BESIII Collaboration), Cross section measurement of $e^+e^- \to K^0_SK^0_L$ at $\sqrt{s} = 2.00$–3.08 GeV, Phys. Rev. D **104**, 092014 (2021).

[123] M. Ablikim *et al.* (BESIII Collaboration), Study of the process $e^+e^- \to \phi\eta$ at center-of-mass energies between 2.00 and 3.08 GeV, Phys. Rev. D **104**, 032007 (2021).

[124] M. Ablikim *et al.* (BESIII Collaboration), Measurement of $e^+e^- \to K^+K^-\pi^0$ cross section and observation of a resonant structure, J. High Energy Phys. 07 (2022) 045.

[125] C. P. Shen *et al.* (Belle Collaboration), Observation of the $\phi(1680)$ and the $Y(2175)$ in $e^+e^- \to \phi\pi^+\pi^-$, Phys. Rev. D **80**, 031101 (2009).

[126] C. P. Shen and C. Z. Yuan, Combined fit to *BABAR* and Belle Data on $e^+e^- \to \phi\pi^+\pi^-$ and $\phi f_0(980)$, Chin. Phys. C **34**, 1045 (2010).

[127] M. Ablikim *et al.* (BESIII Collaboration), Measurement of cross section of $e^+e^- \to \phi\pi^+\pi^-$ at center-of-mass energies $\sqrt{s} = 2.0000$–3.0800 GeV, arXiv:2112.13219.